The determination of the spatial and temporal distribution of Aster Yellows phytoplasma in grapevine

by

Natalie Smyth

Thesis presented in partial fulfillment of the requirements for the degree of Master of Science in Genetics at Stellenbosch University

Supervisor: Prof. Johan T. Burger

Co-supervisor: Dr. Rosineide Souza Richards

March 2015

Declaration

By submitting this thesis electronically, I declare that the entirety of the work contained therein is my own, original work, that I am the authorship owner thereof (unless to the extent explicitly otherwise stated) and that I have not previously in its entirety or in part submitted it for obtaining any qualification.

Date: March 2015

Abstract

South Africa is ranked amongst the top ten for wine production internationally. Viticulture contributes immensely to the economy, which justifies research into the pathogens that may negatively affect wine production. Aster Yellows phytoplasma was reported in South African vineyards in 2010 and has since been an ongoing problem for grape farmers in affected areas. Throughout the world, phytoplasma diseases such as Grapevine Yellows have caused detrimental effects on the vines, often resulting in death. The limited knowledge on prevention and control of the pathogen can be attributed to the lack of full understanding of the epidemiology and accurate diagnosis.

The aim of this study was to determine the spatial distribution of Aster Yellows phytoplasma in individual grapevines and to record a possible temporal or seasonal distribution. The recovery phenotype phenomenon was encountered during the study and surveys were conducted in order to determine whether recovery was permanent. In order to perform the studies, a reliable assay to accurately detect the pathogen in grapevines was required.

A comparison between three assays was completed in furtherance of deciding which to use for the further experimentation. The three assays included a nested PCR utilizing universal primers, a Real-Time PCR using Syto9 as a double stranded DNA specific dye and a Real-Time PCR with a TaqMan® probe using an identical dilution series. Of the three assays tested, the nested PCR proved to be the most sensitive diagnostic procedure, detecting Aster Yellows phytoplasma in very low titers and was thus used for diagnostics in further experiments. In order to determine the spatial patterns of Aster yellows phytoplasma infection, leaf, petiole, trunk, root and cane samples were taken from three whole grapevine plants. Phloem scrapings obtained from the cane samples yielded more positive results in comparison to the other parts of the plant tested. Not only do phytoplasmas display an erratic spatial distribution, but also have a tendency to change over time. Thirty symptomatic grapevines were sampled over one and a half growing seasons, with results concluding that February yielded the most positive diagnoses. Fifty plants that had been previously pruned back and no longer displayed symptoms were also sampled in 2013 and 2014, and all yielded negative results over both years. This study contributes to comprehension of Aster Yellows phytoplasma epidemiology and ultimately the advancement of accurate diagnosis.

Opsomming

Suid-Afrika is internasionaal geposisioneer onder die top tien vir die produksie van wyn. Wingerd dra geweldig by tot die ekonomie, wat navorsing oor die patogene wat wynporduksie negatief beïnvloed, regverdig. Aster Yellows phytoplasmais in 2010 gerapporteer in Suid-Afrikaanse wingerde en is sedertdien 'n deurlopende probleem vir druiweboere in geaffekteerde gebiede. Dwarsdeur die wêreld, het fitoplasma siektes soos Grapevine Yellows ‘n nadelige uitwerking op wingerde, wat dikwels lei tot plantsterftes. Die beperkte kennis oor die voorkoming en beheer van die patogeen kan toegeskryf word aan die gebrek aan begrip van die epidemiologie en akkurate diagnose .

Die doel van hierdie studie was om die ruimtelike verspreiding van Aster geel fitoplasma in individuele wingerdstokke te bepaal en 'n moontlike tydelike of seisoenale verspreiding aan te teken. Die herstel-fenotipe verskynsel is tydens die studie teëgekom en opnames is uitgevoer ten einde te bepaal of die herstel permanent was. Ten einde die studie uit te voer , is 'n betroubare toets vereis om die patogeen in wingerde akkuraat te spoor.

: Drie toetse is vergelyk (en geëvalueer) vir hulle geskikthed vir gebruik in die studie. Die drie toetse het ingesluit 'n geneste PKR wat gebruik maak van universele primers, 'n in-tydse PKR (real-time PCR) wat Syto9 gebruik as 'n dubbelstring DNS spesifieke kleurstof, en 'n in-tydse PKR met 'n TaqMan® peiler, en is vergelyk met behulp van 'n identiese vedunnings reeks. Van die drie toetse , is die geneste PCR bewys om die mees sensitiewe diagnostiese prosedure te wees , en kon Aster geel fitoplasma in baie lae titers opspoor en is dus gebruik vir die diagnose in verdere eksperimente. Ten einde die ruimtelike patrone van Aster geel fitoplasma infeksie te bepaal, is blaar, blaarsteel, stam, wortel en loot monsters van drie volle wingerdstokke geneem. Floëem skraapsels verkry uit die loot monsters het meer positiewe resultate opgelewer in vergelyking met die ander dele van die plant. Nie net vertoon phytoplasmas 'n wisselvallige ruimtelike verspreiding nie, maar het ook 'n neiging om te verander met verloop van tyd. Dertig simptomaties wingerdstokke is versamel oor een en 'n half groeiseisoene,en die resultate het gewys dat Februarie die meeste positiewe diagnoses het. Monsters is versamel in 2013 en 2014 van vyftig plante wat voorheen teruggesnoei is en nie meer simptome vertoon nie, en alle monsters het negatiewe resultate opgelewer oor beide jare. Hierdie studie dra by tot begrip van Aster geel fitoplasma epidemiologie en uiteindelik die bevordering van akkurate diagnose.

List of Abbreviations

AAP	Aquisition Access Period
AGY	Australian Grapevine Yellows
AY	Aster Yellows
BN	Bois Noir
bp	base pair
Ca	*Candidatus*
cv	cultivar
ELISA	enzyme-linked immunosorbent assay
FD	Flavescence dorée
GY	Grapevine Yellows
NCBI	National Centre for Biotechnology Information
PCR	polymerase chain reaction
qPCR	quantitation Real-Time polymerase chain reaction
RFLP	restriction fragment length polymorphisms
rRNA	ribosomal RNA
SAWIS	South African Wine Industry Information and Systems

Acknowledgements

I would like to extend my gratitude to the following people and institutions for their contribution to this study:

- Prof. Johan Burger, for the opportunity to perform this study and for his supervision and guidance.
- Dr. Rosineide Souza Richards, for taking me under her wing, encouraging me to do my best and her intellectual input.
- Dr. Dirk Stephan, for laying down the foundations for this study.
- The entire Vitis laboratory team, for their input, support and advice when times got tough, especially Beatrix Coetzee for sacrificing many working days to come help me sample in Vredendal.
- Winetech, for project funding.
- National Research Foundation (NRF), for personal financial assistance.
- Jeff Joubert and Gert Engelbrecht, for helping me sample in field.
- The farmers in Vredendal, for allowing me to sample in their vineyards.
- Paul and my mother, for their love and never ending encouragement without which my success would not be possible.
- Alex, for the amazing effort you put into helping me with the write-up and not allowing distance to hinder your confidence in me.

Table of Contents

List of Figures

List of Tables

Chapter 1
Introduction

1.1 General Introduction

The South African wine industry is vital to the South African economy. According to the SA Wine Industry Information and Systems (SAWIS) approximately R4 550.9 million was earned in state revenue from wine products. The production of wine in South Africa utilizes over 100 000 hectares of land and provides the employment of 275 606 people. In terms of international wine production, South Africa is ranked ninth with over 1 billion litres produced in 2013. France, Italy and Australia are ranked 2nd, 3rd and 10th respectively and collectively produced over 9 billion litres (www.sawis.co.za).

Phytoplasmas are obligate bacterial parasites, which only replicate and survive intra-cellularily within insect or plant hosts. They are known to cause several diseases in grapevine namely; Bois Noir (BN), Flavescence dorée (FD), Australian grapevine yellows and the focus of this study, Aster Yellows (AY). Internationally, these diseases have caused between 20 – 30% and sometimes as high as 80% loss of yield in vines (Magarey, 1986). Grapevine Yellows (GY), the name given to the group of diseases caused by these pathogens, is known to have detrimental effects in vineyards across the world. The pathogen has induced severe economic losses in the production of wine in Europe and Australia (Lee *et al*, 2000). Since methods of disease control have been implemented, this yield loss has decreased significantly, demonstrating the necessity of research into controlling the pathogen. Recently, Aster Yellows phytoplasma was discovered in the Vredendal and the Wabooms River wine producing areas in South Africa (Engelbrecht *et al*, 2010) which could be pernicious to the country's wine industry. It is thus crucial that different methods of control as well as accurate diagnosis be investigated with the aim of understanding more about phytoplasmas and reducing their ramifications.

Until now, few studies have been performed regarding the spatial and temporal distribution of phytoplasma in plants. In 2004, Christensen and associates recorded that phytoplasma was unevenly distributed in the plants *Catharanthus roseus* and *Euphorbia pulcherrima* and even though it has been suggested that the pathogen is unevenly distributed in grapevine, there is little recorded data that validates this hypothesis (Osler *et al,* 1995). Detecting phytoplasma also depends on seasonal distribution. Terlizzi and Credi (2007) proved that certain

phytoplasma diseases such as Bois Noir was present in grapevine more often in the summer seasons as opposed to the winter seasons in Italy. Many detection methods are able to identify infections, however due to the distributions of the pathogen spatially and temporally, these methods are not always accurate (Belli *et al*, 2010). This is why this research is important as it can contribute to research into more accurate diagnostic assays and thus more effective controlling strategies.

1.2 Project Proposal

The aim of this study was to determine the spatial and temporal distribution of Aster Yellows phytoplasma in grapevine plants. In order to achieve the proposed aim, the following objectives were set out:

- Optimize an established PCR assay to diagnose Aster Yellows phytoplasma in grapevines.
- Collect samples at various time points throughout two grape growing seasons and use an established PCR protocol to determine the seasonal titer fluctuation of Aster Yellows phytoplasma.
- Collect whole plant samples and determine the titer of Aster Yellows phytoplasma in different parts of the plant using PCR.
- Determine whether pruning back grapevine plants induces natural recovery and if this recovery phenotype by testing plants that have been pruned back over a period of 2 years.
- Determine if this natural recovery is true recovery or if it is due to re-infection of Aster Yellows phytoplasma.

1.3 Chapter Layout

Chapter 1: General Introduction, aims and objective of this study and the chapter layout of the thesis is given.

Chapter 2: A synopsis of the general literature related to Aster Yellows phytoplasma in grapevines is provided.

Chapter 3: Investigation into which PCR assay can be used for this research project. Nested PCR and Real-Time PCR are studied.

Chapter 4: The spatial distribution of Aster Yellows phytoplasma is described from results obtained by screening different parts of three whole grapevine plants.

Chapter 5: In this chapter, the temporal/seasonal distribution of Aster Yellows phytoplasma is described from the results obtained by screening the same grapevine plants monthly over the period from November to March. Also, the possibility of inducing the recovery phenotype phenomenon by pruning back infected grapevine plants is investigated.

Chapter 6: General conclusion and future prospects are discussed.

1.4 References

Belli G, Bianco PA, Conti M (2010) Grapevine yellows in Italy: Past, Present and Future. Journal of Plant Pathology 92 (2): 303-326

Christensen NM, Nicolaisen M, Hansen M, Schulz A (2004) Distribution of Phytoplasmas in Infected Plants as Revealed by Real-Time PCR and Bioimaging. *Molecular Plant Microbe Interactions* 17 (11): 1175-1184

Engelbrecht M, Joubert J, Burger JT (2010) First report of aster yellows phytoplasma in grapevines in South Africa. *Plant Disease* 94 (3): 373

Lee IM, Davis RE, Gundersen-Rindal DE (2000) Phytoplasma: phytopathogenic mollicutes. Annual Review of Microbiology 54: 221-255

Magarey PA (1986) Grapevine Yellows – Aetiology, epidemiology and diagnosis. South African Journal of Enology and Viticulture 7 (2): 90-100

SA Wine Industry Statistics nr 37 (2013) SA Wine Industry Information & Systems, SAWIS, PO Box 238, Paarl 7620

Terlizzi F, Credi R (2007) Uneven distribution of stolbur phytoplasma in Italian grapevines as revealed by nested-PCR. *Bulletin of Insectology* 60 (2): 365-366

Chapter 2
Literature Review

2.1. Introduction

The first known encounter of the peculiar bacterium, phytoplasma, was in ancient China, where plants were deliberately infected in order to induce a change of colour in the leaves and blossoms. These plants were used as decorations and were highly sought after (Strauss, 2009). Unfortunately, phytoplasmas are now less desirable and more abundant, causing devastation in a wide range of crops. In South Africa it is known to shrivel the grapes on grapevines, reduce corn size in South America, kill apples and pears in the United States of America and Europe and can also cause deterioration in peanuts, soybean and sesame seeds in Asia. Pear decline, a disease caused by phytoplasma, was first reported during the Second World War, and is known to reduce the size of the fruit significantly (Bertaccini, 2007). Outbreaks of phytoplasmas in apple fruits alone have caused detrimental economical losses in countries such as Japan and Germany (Strauss, 2009).

Considering the devastation phytoplasmas can cause in crops, it was surprising to note that research of this pathogen started off slow, especially considering their economic importance (Alma *et al*, 1997). Scientists initially believed that it was a virus that caused the diseases in the crops due to its infectious nature and the ability to infect plants through insect vectors (Bertaccini, 2007). Attempts to fulfil Koch's postulates have repeatedly failed, as even today the bacterium remains unculturable *in vitro* in cell-free media (Strauss, 2009).

Grapevines (*Vitis vinifera)* are one of many plant hosts of phytoplasmas (Engelbrecht *et al*, 2010). Grape related products such as wine are widely produced around the world and thus are economically important. South Africa, in particular, is ranked ninth in the world with regards to wine production (SA Wine Industry Statistics nr 38, 2014). The diseases caused by phytoplasmas in grapevines such as Grapevine Yellows disease, Flavescence dorée and Bois Noir cause a noticeable decline in plant health and ultimately wine production. Loss of yield has been recorded to be as high as 80% in phytoplasma infected vines (Magarey, 1986). Research involving control of these diseases is paramount and factors that influence control include accurate diagnosis, vector control and a full understanding of the pathogen.

2.2. Phytoplasmas

2.2.1. Discovery

The earliest description known of a phytoplasma disease was in the Song Dynasty in China, more than a millennium ago. Peonies are a flowering plant that was used as decoration in this period, however it was the phytoplasma-infected, "Yao-yellow kind" peonies that were widely acclaimed and were described as the most beautiful tree peonies, despite being less vigorous and unable to produce seeds (Maramorosch, 2011).

In 1926, L.O. Kunkel proved that the transmission of phytoplasmas from plant to plant occurred through the leafhopper, *Macrosteles fascifrons*. He subsequently concluded that the pathogen was of viral etiology as he was unable to observe any viable bacteria or fungi in diseased plants (Kunkel, 1926). Approximately 30 years later, Karl Maramorosch performed an experiment using tetracycline. He recorded the effects of this antibiotic by injecting it into infected leafhoppers. It was concluded that the insects were unable to transmit the disease; but that this was not due to the antibiotic but due to the heat in the greenhouse in which the experiment was performed. Maramorosch published these results despite knowing the antibiotics have no effect on viruses (Maramorosch, 1958).

The breakthrough discovery was when Japanese scientists detected what they termed as Mycoplasma-like organisms (MLOs) in diseased plants and insects in 1967 (Doi *et al,* 1967). Mycoplasmas are bacteria that are parasitic in nature and do not have cell walls. However, unlike mycoplasmas which cause many disorders in humans and animals, phytopathogenic MLOs are still unculturable in cell-free media despite many attempts (Contaldo *et al*, 2012). At the 10th Congress of the International Organization of Mycoplasmology, the pathogen was renamed as phytoplasma by the Phytoplasma Working Team in 1994 (Lee *et al*, 2000).

2.2.2. Characteristics and Classification

Doi *et al* (1967) used ultrathin cuttings of the phloem of phytoplasma infected plant tissue and observed the organisms under an electron microscope. Their findings showed organisms that were pleomorphic and instead of having a cell wall, they were encapsulated by a thin, single unit membrane. Phytoplasmas are divergent from gram positive bacteria in the *Bacillus*/*Clostridium* group. They belong to the class *Mollicutes* and have a small genome ranging from 680 to 1600kb (Contaldo *et al*, 2012). The cells are approximately 500 nm in

diameter (Lee *et al*, 1998). Phytoplasmas demonstrate an independent metabolism allowing them to thrive in trans-kingdom environments such as the phloem in plants and the haemolymph in insects (Contaldo *et al*, 2012).

Characterization of phytoplasmas has proven difficult due to the inability to be cultured in cell-free media thus Koch's postulates have not been achieved. However, DNA-based technologies and sequencing of ribosomal rRNA allowed for classification under the *Mollicutes* class (Bertaccini, 2007). Phytoplasmas are genetically diverse from mycoplasmas that infect animals because of the spacer region that is found between the 16S and 23S ribosomal regions. Using PCR and RFLP analyses, sequences in the 16S rRNA were amplified and used to differentiate a wide range of phytoplasma species (Bertaccini, 2007). Phytoplasmas can therefore be classified according to the sequence of their specific 16S rRNA (for those where sequence was available). Woese (1987) proposed using the conserved 16S rRNA gene as a universal marker for phylogenetic studies specific to classifying and diagnosing prokaryotes. This has been successfully used in studies determining the relationships between mollicutes and bacteria with cell walls (Weisburg *et al*, 1989). The 16S rRNA genes of 37 characteristic strains of phytoplasma were sequenced by Namba *et al*. (1993), Gunderson *et al*. (1994) and Seemüller *et al.* (1994), allowing comparative studies. These comparisons showed that the species' 16S rRNA sequences were more similar to each other than any other prokaryote. The conclusion was made that phytoplasmas should be classified in their own monophyletic clade of organisms, but this clade, however, is more closely related to *Mollicutes* rather than bacteria with cell walls (Seemüller *et al,* 1998).

Following the conclusion of these studies, the International Committee of Systematic Bacteriology (ICSB) Subcommittee on the taxonomy of *Mollicutes* (1993, 1997) officially changed the name from MLOs to Phytoplasma and was to be grouped under taxonomic status *Candidatus* (Murray and Schleifer, 1994). Phytoplasmas are classified in different phylogenetic groups and subgroups according to the sequence of their ribosomal DNA and other conserved genes.The table below (Table 2.1) depicts the *Candidatus* phytoplasma species classified according to RFLP analyses done on the 16S rRNA gene, giving the 16S rRNA group (Roman numeral) and subgroup (letter), the GenBank accession number and the formal/informal scientific name.

Table 2.1: 16S rRNA RFLP group-subgroup classification and '*Candidatus* Phytoplasma' species. Rows highlighted in black are those phytoplasma that affect grapevine. (Dr RE Davis, Unites States Department of Agriculture, Phytoplasma Resource Centre)

Phytoplasma/disease common name[1]	16S rDNA group-subgroup	GenBank no.	Named '*Candidatus* Phytoplasma' species	Informally proposed '*Candidatus* Phytoplasma' species[2]
Aster yellows (AY)	16SrI	M30790	'*Candidatus* Phytoplasma asteris'	
WB disease of lime	16SrII-B	U15442	'*Ca.* Phytoplasma aurantifolia'	
Papaya yellow crinkle	16SrII-D	Y10097	'*Ca.* Phytoplasma australasiae'	
Western X-disease	16SrIII-A	L04682	'*Ca.* Phytoplasma pruni'	
Palm lethal yellowing	16SrIV-A	U18747		'*Ca.* Phytoplasma palmae'
Elm yellows	16SrV-A	AY197655	'*Ca.* Phytoplasma ulmi'	
Jujube WB	16SrV-B	AB052876	'*Ca.* Phytoplasma ziziphi'	
Flavescence dorée	16SrV-C	AF176319		'*Ca.* Phytoplasma vitis'
Clover proliferation	16SrVI-A	AY390261	'*Ca.* Phytoplasma trifolii'	
Ash yellows	16SrVII-A	AF092209	'*Ca.* Phytoplasma fraxini'	
Loofah WB	16SrVIII-A	AF086621		'*Ca.* Phytoplasma luffae'
Almond lethal disease	16SrIX-D	AF515636	'*Ca.* Phytoplasma phoenicium'	
Apple proliferation	16SrX-A	AJ542541	'*Ca.* Phytoplasma mali'	
Pear decline	16SrX-C	AJ542543	'*Ca.* Phytoplasma pyri'	
Spartium WB	16SrX-D	X92869	'*Ca.* Phytoplasma spartii'	
European stone fruit Y	16SrX-F	AJ542544	'*Ca.* Phytoplasma prunorum'	
Rice yellow dwarf	16SrXI-A	AB052873	'*Ca.* Phytoplasma oryzae'	
Stolbur phytoplasma	16SrXII-A	AF248959	'*Ca.* Phytoplasma solani'	

Phytoplasma/disease common name[1]	16S rDNA group-subgroup	GenBank no.	Named '*Candidatus* Phytoplasma' species	Informally proposed '*Candidatus* Phytoplasma' species[2]
Australian GY	16SrXII-B	Y10097	'*Ca.* Phytoplasma australiense'	
Hydrangea phyllody	16SrXII-D	AB010425	'*Ca.* Phytoplasma japonicum'	
Strawberry yellows	16SrXII-E	DQ086423	'*Ca.* Phytoplasma fragariae'	
Mexican periwinkle Vir	16SrXIII-A	AF248960		No '*Candidatus*' name proposed
Bermuda grass WL	16SrXIV	AJ550984	'*Ca.* Phytoplasma cynodontis'	
Hibiscus WB	16SrXV	AF147708	'*Ca.* Phytoplasma brasiliense'	
Sugarcane yellow leaf	16SrXVI	AY725228	'*Ca.* Phytoplasma graminis'	
Papaya bunchy top	16SrXVII	AY725234	'*Ca.* Phytoplasma caricae'	
Potato purple top wilt	16SrXVIII	DQ174122	'*Ca.* Phytoplasma americanum'	
Chestnut WB	16SrXIX	AB054986	'*Ca.* Phytoplasma castaneae'	
Buckthorn WB	16SrXX	X76431	'*Ca.* Phytoplasma rhamni'	
Pine shoot proliferation	16Sr XXI	AJ632155	'*Ca.* Phytoplasma pini'	
Nigerian Awka disease	16Sr XXII-A	Y14175		'*Ca.* Phytoplasma cocosnigeriae'
Buckland Valley GY	16SrXXIII-A	AY083605		No '*Candidatus*' name proposed
Sorghum bunchy shoot	16SrXXIV-A	AF509322		No '*Candidatus*' name proposed
Weeping tea WB	16SrXXV-A	AF521672		No '*Candidatus*' name proposed
Sugarcane yellows phytoplasma D3T1	16SrXXVI-A	AJ539179		No '*Candidatus*' name proposed
Sugarcane yellows phytoplasma D3T2	16SrXXVII-A	AJ539180		No '*Candidatus*' name proposed

Phytoplasma/disease common name[1]	16S rDNA group-subgroup	GenBank no.	Named '*Candidatus* Phytoplasma' species	Informally proposed '*Candidatus* Phytoplasma' species[2]
Derbid phytoplasma	16SrXXVIII-A	AY744945		No '*Candidatus*' name proposed
Cassia italica WB	16SrXXIX	EF666051	'*Ca.* Phytoplasma omanense'	
Salt cedar WB	16SrXXX	FJ432664	'*Ca.* Phytoplasma tamaricis'	
Allocasuarina yellows	Undetermined	AY135523	'*Ca.* Phytoplasma allocasuarinae'	
Parsley leaf of tomato	"	EF199549	'*Ca.* Phytoplasma lycopersici'	
Tanzanian lethal disease	"	X80117		'*Ca.* Phytoplasma cocostanzaniae'
Chinaberry yellows	"	AF495882		No '*Candidatus*' name proposed

[1]Abbreviations in table are listed as: AY, aster yellows; WB, witches'-broom; Y, yellows; GY, grapevine yellows; Vir, virescence; WL, white leaf.
[2]Names not been formally published

2.2.3. Lifecycle

Phytoplasmas have a dual lifecycle as they have the ability to replicate in both plants and insects (Lee *et al*, 2000). The pathogen inhabits the phloem tissues in the plant host, including the mature sieve tubes that do not have nuclei and the young phloem cells that still have their nuclei (Hogenhout *et al*, 2008). Within the insect hosts, the phytoplasma replicates in various tissues, however, the pathogen must cross into the salivary glands in order to ensure introduction into plant hosts (Hogenhout *et al*, 2008).

The duel life cycle is depicted in Figure 2.1. The acquisition feeding at stage 1 shows a healthy leafhopper feeding on a plant infected with phytoplasma. The uptake of the phytoplasma occurs through the phloem into the insect's stylet and travels though the intestine where it finally enters the circulatory system of the haemolymph. During stage 2 (the latency period), the phytoplasmas replicate within the infected insect and then colonizes the salivary glands (Christensen *et al,* 2005). The insect is regarded as infectious when the pathogen has travelled through the salivary glands. The cells within the salivary glands need to be in high abundance in order to do so. The high titer can provide an indication of how efficient the transmission is (Weintraub and Jones, 2010). High levels of phytoplasma cells

must amass in the salivary glands, specifically in the posterior acinar cells. If the phytoplasma cells fail to migrate in or out of the posterior acinar cells, the vector is classified as a dead-end host (Weintraub and Beanland, 2006). This stage of the lifecycle lasts approximately 3 weeks, after which the insect remains infected throughout its entire lifetime. In stage 3, the phytoplasmas are transmitted into a new healthy plant via inoculation feeding. The phytoplasmas then multiply within the new plant host (Christensen *et al,* 2005).

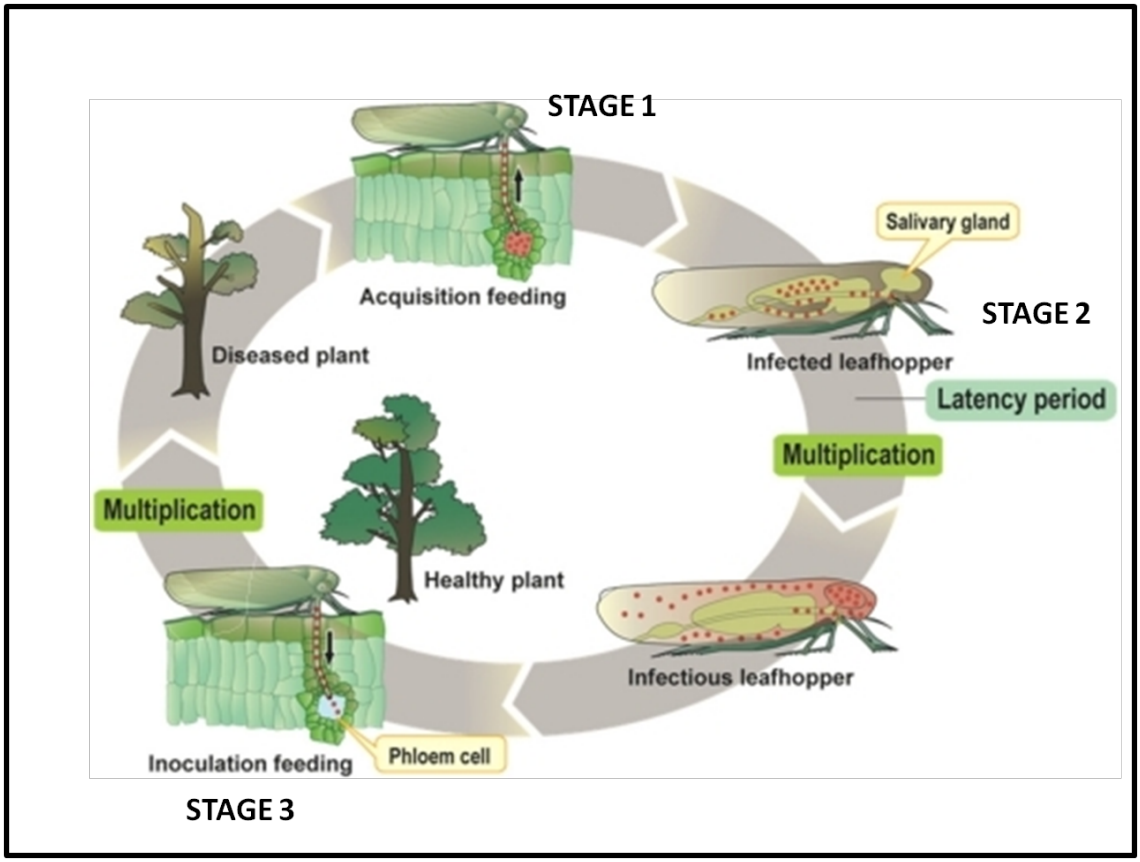

Figure 2.1: The duel life cycle of phytoplasma in three stages, from the diseased plant, to infection of a leafhopper then finally to infection of a healthy plant. Adapted from Oshima *et al* (2011).

2.2.4. Plant Hosts

Phytoplasma infects a wide range of plants, with over 100 seed plant species documented (Lee *et al,* 2000). This is an important characteristic for the epidemiology of the pathogen's diseases (Christensen *et al*, 2005). Plant hosts include species such as apple, periwinkle, potato, lettuce, celery, carrots and grapevines (Lee *et al*, 2000), and causes diseases such a Grapevine Yellows, Bois Noir, Flavenscence Dorée, Apple Proliferation, Coconut Lethal Yellowing and Peach X-disease (Bertaccini and Duduk, 2009).

Phloem tissue, which is responsible for nutrient transport within the plant, is the target of infection by phytoplasma (Lee *et al,* 2000). Due to the abundance of phloem within a plant host, phytoplamas can be detected in most organs (Christensen *et al*, 2005). Phytoplasma do not possess flagella or cilia for active transport and therefore passive movement through the plants sieve tube elements was suggested as the mode of transport by Christensen *et al* (2005). The pathogen moves in the direction of the phloem stream, from the source tissue (the source of nutrients such as sucrose) towards the sink tissues (tissues that absorb the nutrients). This movement however, is slower than that of the solutes (Christensen *et al*, 2004). Little is known regarding the interaction between the plant host and the phytoplasma, nevertheless, several studies have shown that the pathogen can alter the levels of the endogenous phytohormones within the plant (Christensen *et al*, 2004).

Infection titers between plants are known to differ greatly. Plant hosts such as grapevines and elms (genus *Ulmus*) typically have low infection titers and difficulty often arises when trying to detect the phytoplasma using microscopy methods and molecular assays. Plants including apple trees (*Malus domestica*) and periwinkle (genus *Vinca*) have yielded high infection titers (Berges *et al*, 2000) and are therefore often used for molecular research involving phytoplasmas. It was suggested that different levels of pathogenicity exist in different hosts which could explain the vast difference in infection titers (Berges *et al*, 2000).

2.2.4.1. Phytoplasmas in South African Vineyards

Vitis vinifera, the common grapevine, can be infected by a wide range of phytoplasmas, specifically Bois Noir, Flavescence dorée, Australian Grapevine Yellows phytoplasma and, the focus of this research project, Aster Yellows phytoplasma. The first report of mixed phytoplasma infection in South African grapevines was in 2006 by Botti and Bertaccini. Profiles of Stolbur phytoplasma (ribosomal subgroup 16SrXII-A) and *Candidatus* Phytoplasma aurantifolia (ribosomal subgroup 16SrII-B) were found in samples collected. In 2010, Aster Yellows phytoplasma was first reported in South African vineyards by Engelbrecht *et al*. It was found in the Vredendal and Wabooms River area, and later in 2010, vineyards in Roberston and Trawal showed infection as well (Douglas-Smit *et al*., 2010). There are ongoing studies in all of these areas, including a recently completed project involving the incidence and distribution of phytoplasma in a vineyard (Carstens, 2014).

2.2.5. Insect Hosts

The insect hosts responsible for the spread of phytoplasma diseases are phloem-sucking leafhoppers (Lee *et al*, 2000). A variety of phytoplasmas can be transmitted by several different species of leafhopper, including aster yellows phytoplasma which is transmitted by approximately 24 leafhopper species (Seemüller *et al*, 2002 and Lee *et al*, 2003). Individual species are also able to transmit different strains of phytoplasma (Nielson, 1979). The order into which these insects are classified is the Hemiptera – it possesses several characteristics that allow it to be the optimal vector for phytoplasma transmission, namely; (1) both adults and young are able to transmit the bacteria, (2) they feed on the phloem tissue of the plant only, allowing easy transmission of phytoplasma, (3) they have a propagative and consistent relationship with the pathogen and (4) the insects have obligate symbiotic prokaryotes that are passed on to offspring during reproduction using the same mechanisms that allow the transovarial infection of offspring. It is known that insect vectors vary greatly, but transmission does not depend on the strain of the phytoplasma, rather on the species of the insect and how they feed (Weintraub and Bealand, 2006).

Transmission of Aster Yellows phytoplasma can be influenced by the sex of the leafhopper. Experiments in both greenhouse and laboratory conditions have determined that male leafhoppers were more likely to be infected by the pathogen, but females were shown to transmit more easily (Beanland *et al*, 1999). Transmission of Aster Yellows phytoplasma by the separate genders of leafhoppers depends on the time of year. Beanland e*t al* (2005) determined that female leafhoppers inoculated phytoplasmas more often early in the season; however males tended to be more active throughout the growing season. Both of the previous studies were performed on the leafhopper species, *Macrosteles quadrilineatus* Forbes, a well known vegetable crop pest that is classified as the primary vector of Aster Yellows phytoplasma in Midwestern parts of the world (Frost *et al*, 2011).

In 2011 Krüger *et al* found that the leafhopper transmitting Aster Yellows phytoplasma in South Africa was the species, *Mgenia fuscovaria.* Affected vineyards were surveyed for two years for species of planthoppers and leafhoppers. All specimens collected were tested for Aster Yellows phytoplasma infection and subsequently, transmission experiments were performed. This led to the final identification of *M. fuscovaria* (Krüger *et al*, 2011) and thus allowed further research into behavioural analyses and epidemiology studies.

Investigations have been done on the effect of phytoplasma infection on the insect vector. Several leafhopper species are negatively affected by the pathogen as they die a few weeks after initial infection, whereas other species are known to benefit from the infection as they live longer, specifically when their main food source is lacking or when living in suboptimal temperatures (Hogenhout *et al*, 2008). Behavioural studies show that the leaf hoppers prefer to feed from already infected grapevine plants. Healthy plants and infected plants were placed in a controlled environment and it was observed that there were more instances where the insects were attracted to the grapevines already infected with phytoplasma (Krüger, 2012). Further explanations as to why this happens is currently being explored.

2.2.6. Symptoms

In contrast to the insect vectors, plant hosts are negatively affected by phytoplasma infection. In general, most plant hosts that are infected show stunted growth and may not produce flowers, fruits or seeds (Hogenhout *et al*, 2008). When the flower does grow, it may show virescence and phyllody (Christensen *et al*, 2005). Leaf yellowing is an important symptom often used to diagnose plants. It is a common symptom and is thought to be caused by a change in carbohydrate synthesis and transportation (Bertaccini and Duduk, 2009).

Symptoms of Aster Yellows phytoplasma infection in grapevine include yellowing of the leaves (Figure 2.2A), shortening of internodes, lack of cane lignification and downward rolling of leaves (Engelbrecht *et al*, 2010 and Botti and Bertaccini, 2006). Although the mechanism in which the host plant and the phytoplasmas interact is not fully understood, the change in the levels of the endogenous phytohormones within the plant can cause propagation of axillary shoots (Figure 2.2B) and abnormal pigmentation (Christensen *et al*, 2004).

Figure 2.2: Symptoms of Aster Yellows phytoplama infection in grapevine plants. (A) Abnormal pigmentation. (B) Propagation of axillary shoots. (C) Aborted bunches.

The range of symptoms and severity of expression of Grapevine Yellows disease tends to show seasonal patterns. During the Spring months, phytoplasma infected grapevines show abnormal sprouting, and when summer begins, the leaves change from green to yellow (in white grape cultivars) or purple in colour (red grape cultivars) and start to roll downwards in plants with Flavescence dorée (Belli *et al,* 2010). The fruit start to dry up (Figure 2.2C) and the canes remain green and tend to droop. Symptoms can also be restricted to a certain part of the grapevine plant, for example, may only occur on one branch or several canes while the rest of the plant appears to be healthy. The symptoms would be the result of infection from the previous season (Belli *et al*, 2010). In cultivars that are particularly susceptible to phytoplasma such as Chardonnay, death will occur after a few years (Carstens, 2014).

2.2.7. Control Strategies and Treatment

Unfortunately, once a plant has been infected by any phytoplasma species, including Aster Yellows phytoplasma, there is no scientifically proven way in which the plant can be cured. This then requires the prevention of infection or the spread of disease throughout a crop, specifically vineyards. Carstens (2008) suggested four ways in which to control the spread of aster yellows phytoplasma in vineyards.

1. The plant/s that appears to be the source of infection should be removed from the vineyard immediately.
2. Vineyards should be maintained in terms of removing weeds and surrounding plants as they could serve as a host plant during the winter months.

3. When planting new grapevines into a vineyard, ensure that they are healthy by running diagnostic tests before planting.
4. Leafhoppers should be chemically controlled by using insecticides.

There are several practices that are being investigating that can be used to control phytoplasma infection in crops:

2.2.7.1. Induction of Recovery and Minimizing Disease Inoculum

Recovery phenotype is the spontaneous remission of phytoplasma symptoms (Caudwell, 1961). This was first observed in France and Italy in grapevines that were infected with Flavescence dorée (grapevine yellows disease) (Musetti *et al*., 2007). There have been many theories regarding how recovery occurs, which include the increase of hydrogen peroxide in the plants (Musetti *et al*., 2004). It can also be induced by deliberate stresses such as grafting, cutting back and replanting (Osler *et al*., 1993). Bois Noir infected plants were successfully reduced by utilizing pruning methods and pollarding in Austrian vineyards. These pruning and pollarding measures induced recovery, however, duration of recovery was influenced by severity of infection and the age of the grapevine (Riedle-Bauer, 2009).

The recovery can be permanent or temporary and a plant is considered to be in permanent recovery when it has not presented symptoms of phytoplasma infection for approximately three consecutive years (Maixner, 2006). There has been no scientific evidence regarding the reliability of permanent recovery in grapevines.

2.2.7.2. Vector Control

A common practise used to control phytoplasmas is the use of chemical insecticides in order to reduce the presence of the insect vectors in vineyards. The type of insecticide and the time of application can influence the efficiency (Carstens, 2014). Saracco *et al* (2008) tested the activity of different chemicals used as insecticides at different times, focussing on the prevention of the transmission of chrysanthemum yellows phytoplasma by leafhoppers. It was found that neonicotinoid imidacloprid showed the highest capacity in preventing transmission. Conclusions highlighted that insecticides are not always reliable in both containing populations and preventing transmission (Saracco *et al*, 2008). Insect-proof netting has shown success in preventing phytoplasma transmission in foundation vineyards in Italy (Mannini, 2007). Howard *et al* (1998) suggested using mulching as a way to prevent insects from transmitting diseases to crops by repelling them. In South Africa, a practise of

severe pruning has been established and is followed directly by application of insecticides (Carstens, 2014).

2.2.8. Detection and diagnosis

2.2.8.1. Previous detection methods

As phytoplasmas are incapable of being cultivated *in vitro* in any cell-free media, molecular-based detection methods are used, before which observation of symptoms was used to diagnose plants (Lee *et al*, 2000). Electron microscopy was also used to look for the bacteria in ultra-thin cuttings of the phloem tissue (Bertaccini and Duduk, 2009). In the 1980s, serological tests such as enzyme-linked immunosorbent assay were used for detection. This technique used highly specific monoclonal antibodies and was relatively simple and accurate; however it only detected specific strains of phytoplasma (Lee *et al*., 2000).

Molecular-based detection such as PCR-based assays were developed later on in the 1980s, using both generic and specific primers. The generic primers failed to detect low titers of the pathogen, but the specific primers, designed based on the conserved 16S rRNA gene sequences, proved more accurate (Lee *et al*., 2000). Currently, the industry makes use of a nested PCR, also using primers based on the 16S rRNA gene sequences (Clair *et al*., 2003). RFLP analysis of the PCR products is required to differentiate phytoplasmas that belong in subgroup 16SrV-A from phytoplasmas associated with Flavescence doree (Bianco *et al*., 2004).

2.2.8.2. Real Time PCR

In 2004, Christensen and associates developed a Real-Time PCR assay and a bioimaging method that were able to quantify a wide range of phytoplasma strains. The Real-Time PCR assay used the 16S ribosomal gene and was used to study the distribution of phytoplasma in infected plants, specifically *E. pulcherrima* and *C. roseus*.

A quantitative PCR assay was developed by Marzachi and Bosco (2005) that used the 16S rDNA target sequence of the phytoplasma that causes Chrysanthemum Yellows. Angelini *et al* (2007) developed a new TaqMan Real-Time PCR assay for detecting phytoplasmas associated with grapevine yellows. Further research led to the development of a multiplex Real-Time PCR, utilizing primers and probes designed to amplify a region of the 23S rRNA. This assay is able to detect phytoplasmas from all groups whilst simultaneously identifying

specifically phytoplasmas in group 16SRI (Hodgetts *et al*, 2009). Diagnosing phytoplasmas in plant hosts using Real-Time PCR is constantly being improved with promising results. Difficulties that tend to arise include very low titers that do not allow sufficient amplification and yield negative results. Overcoming this obstacle is essential as quantifying infection titers can give rise to further understanding of phytoplasmas.

2.2.9. Spatial Distribution in a vineyard

The spatial distribution of a specific disease is defined as how the pathogen spreads in space (Carstens, 2014). Studying the spatial pattern of diseases can give rise to knowledge regarding the epidemiology and disease control. There have been several studies involving the spatial pattern of phytoplasmas in crops around the world. The spatial distribution of X-disease in sweet cherry trees was analyzed in California in 1998 by Uyemoto *et al*. The pattern appeared to be random and there were indications of secondary spread aggregated around infected plants. Removal of trees together with insecticide application lowered the rate of new infections significantly (Uyemoto *et al*, 1998).

A random pattern was also found in Bois Noir infected vineyards in Italy. However, there was a clustering of diseased grapevines where nettle surrounded the edge of the vineyards. This provided evidence that surrounding vegetation could influence the spread of the disease and cannot be overlooked as hosts (Mori *et al*, 2008).

PATCHY (spatial analysis software) analysis was performed on vineyards severely infected with Aster Yellows phytoplasma in Vredendal, South Africa. Surveys were conducted on affected vineyards and results yielded a non-random clustering with most of the diseased plants situated on the edges of vineyards (Carstens, 2014). Several symptomless vines infected with Aster Yellows phytoplasma were also found during the survey, while vines that displayed distinct symptoms yielded negative results. It was suggested that there may be a spatial distribution of the pathogen within individual plants (Carstens, 2014).

2.2.10. Spatial Distribution in individual plants

It has been suggested in many studies that phytoplasmas adopt a spatial distribution within their plant hosts, and that infection titers are not uniform in all of the plant organs. Further research has been contradictory, with results that yield petioles with the highest pathogen titer and others concluding leaf material yields the highest titer (Christensen *et al*, 2004; Terlizzi

and Credi, 2007). However, these studies involve different plant hosts, as well as different *Candidatus* species. There have been few studies involving Aster Yellows phytoplasma infection in grapevine with regards to the spatial patterns it may exhibit. One of which include analyses on canes with the leaves and petioles, concluding that the nodes on the canes revealed most positive results (Spinas, 2012). As this study was limited to the canes, further research on the entire plant is required to finalize a spatial pattern of Aster Yellows phytoplasma in grapevines.

2.2.11. Temporal/Seasonal Distribution

Infection titers not only exhibit spatial patterns, but also tend to change over time. Symptom expression changes in severity throughout the season, suggesting that phytoplasmas have a temporal distribution (Belli *et al*, 2010). Phytoplasmas such as Bois Noir have shown to be present more often in the summer seasons than the winter seasons. A study in Italy using nested PCR assays provided evidence to this theory (Terlizzi and Credi, 2007). According to research by Constable *et al* (2003), Australian Grapevine Yellows exhibited higher infection titers in January and February in Australia. It was suggested that sampling for diagnostic purposes should occur in this period for greater accuracy (Constable *et al*, 2003). Further surveys of the wineland districts in Australia showed that the pathogen was found more in the warmer inland areas of New South Wales when compared to other states. This may imply that climate influences the temporal distribution (Constable *et al*, 2003).

There is also an indication that infection incidence may increase over time. Batlle *et al* (2000) observed an increase of incidence of Bois Noir in Spanish vineyards. Surveys performed in Vredendal, South Africa also provided evidence of a severe increase of incidence of Aster Yellows phytoplasma in grapevines, especially in the Chardonnay cultivar (Carstens, 2014).

Further understanding on the temporal distribution is required as accurate diagnosis can be influenced by when diseased plants are sampled.

2.3. References

Alma A, Bosco D, Danielli A, Bertaccini A, Vibio A, Arzone A (1997) Identification of phytoplasmas in eggs, nymphs and adults of Scaphoideus titanus Ball reared on healthy plants. Insect Molecular Biology 6:115-121

Angelini E, Bianchi GL, Filippin, L, Morassutti C, Borgo M (2007) A new TaqMan® method for the identification of phytoplasmas associated with grapevine yellows by real-time PCR assay. Journal of Microbial Methods 68: 613-622

Batlle A, Martinez MA, Lavina A (2000) Occurrence, distribution and epidemiology of Grapevine Yellows in Spain. European Journal of Plant Pathology 106: 811–816

Beanland L, Hoy CW, Miller SA, Nault LR (1999) Leafhopper (Homoptera: Cicadellidae) transmission of aster yellows phytoplamsa: Does gender matter? Environ. Entomol. 28:1101-1106

Belli G, Bianco PA, Conti M (2010) Grapevine yellows in Italy: Past, Present and Future. Journal of Plant Pathology 92 (2): 303-326

Berges R, Rott M, Seemüller E (2000) Range of Phytoplasma Concentrations in Various Plant Hosts as Determined by Competitive Polymerase Chain Reaction. Bacteriology 90 (10): 1145-1152

Bertaccini A (2007) Phytoplasmas: diversity, taxonomy, and epidemiolgy. Frontiers in Bioscience 12: 673-689

Bertaccini A, Duduk B (2009) Phytoplasma and phytoplasma diseases: a review of recent research. Phytopathologia Mediterranea 48:355–378

Botti S, Bertaccini A (2006) First report of phytoplasmas in grapevine in South Africa. Plant Disease 90: 1360

Carstens R (2008) Aster yellows disease in vineyards in South Africa. Wineland 228:90-91

Carstens R (2014) The incidence and distribution of grapevine yellows disease in South African vineyards. MSc thesis. Stellenbosch University

Caudwell, A (1961) Les phénomènes de rétablissement chez la flavescence dorée de la vigne. Annales des Epiphyties 12: 347-354

Christensen NM, Nicolaisen M, Hansen M, Schulz A (2004) Distribution of Phytoplasmas in Infected Plants as Revealed by Real-Time PCR and Bioimaging. Molecular Plant Microbe Interactions 17 (11): 1175-1184

Christensen NM, Axelsen KB, Nicolaisen M, Schulz A (2005) Phytoplasmas and their interactions with hosts. Trends in Plant Science 10(11): 526-535

Clair D, Larrue J, Aubert G, Gillet J, Cloquemin G, Bodoun-Padieu E (2003) A multiplex nested-PCR assay for sensitive and simultaneous detection and direct identification of a phytoplasma in the Elm yellows group and Stolbur group and its use in survey of grapevine yellows in France. Vitis 42: 151-157

Constable FE, Gibb KS, Symons RH (2003) Seasonal distribution of phytoplasmas in Australian grapevines. Plant pathology 52: 267-276

Contaldo N, Bertaccini A, Paltrinieri S, Windsor HM, Windsor GD (2012) Axenic culture of plant pathogenic phytoplasmas. Phytopathologia Mediterranea 51 (3): 607-617

Doi Y, Teranaka M, Yora K, Asuyama H (1967) Mycoplasma- or PLT group-like microorganisms found in the phloem elements of plants infected with mulberry dwarf, potato witches‟ broom, aster yellows or paulownia witches‟ broom. Annual Phytopathology Society of Japan 33: 259-266

Engelbrecht M, Joubert J, Burger JT (2010) First report of aster yellows phytoplasma in grapevines in South Africa. Plant Disease 94 (3): 373

Frost KE, Willis DK, Groves RL (2011) Detection and variability of Aster Yellows phytoplasma titer in its insect vector, *Macrosteles quadrilineatus* (Hemiptera: Cicadellidae). J. Econ. Entomol. 104 (6): 1800-1815

Gundersen DE, Hammond RW, Davis RE (1994) Use of mycoplasmalike organism (MLO) group specific oligonucleotide primers for nested PCR assays to detect mixed MLO-infections in a single host plant. Phytopathology 84: 559-566

Hogenhout SA, Oshima K, Ammar E-D, Kakizawa S, Kingdom HN, Namba S (2008) Phytoplasmas: Bacteria that manipulate plants and insects. Molecular Plant Pathology 9: 403-423

Hodgetts J, Boonham N, Mumford R, Dickinson M (2009) Panel of 23S rRNA gene-based Real-Time PCR assays for improved universal ad group-specific detection of phytoplasmas. Applied and Environmental Microbiology 75 (9): 2945-2950

Kunkel LO (1926) Studies on aster yellows. American Journal of Botany 23: 646-705

Krüger K (2012) Manipulation of insect vector behaviour by aster yellows phytoplasma: potential for vector control. Minutes of the Winetch Grapevine Virus Workshop XI held a Infruitec, Stellenbosch

Krüger K, de Klerk A, Douglas-Smit N, Joubert J, Pietersen G, Stiller M (2011) Aster yellows phytoplasma in grapevines: identification of vectors in South Africa. Bulletin of Insectology 64 (Supplement): S137-S138

Lee I-M, Gundersen-Rindal DE, Bertaccini A (1998) Phytoplasma: Ecology and Genomic Diversity. Phytopathology 88 (12): 1359-1366

Lee I-M, Davis RE, Gundersen-Rindal DE (2000) Phytoplasma: phytopathogenic mollicutes. Annual Review of Microbiology 54: 221-255

Magarey PA (1986) Grapevine Yellows – Aetiology, epidemiology and diagnosis. South African Journal of Enology and Viticulture 7 (2): 90-100

Maixner M (2006) Temporal behaviour of grapevines infected by type II of Vergilbungskrankheit (Bois noir). Extended Abstracts 15th Meeting of ICVG Stellenbosch 2006: 223-224

Maramorosch K (1958) Viruses that infect and multiply in both plants and insects. Transactions New York Academy Sciences (Serie II) 20: 383-395

Maramorosch K (2011) Historical reminiscences of phytoplasma discovery. Bulletin of Insectology (Supplement): S5-S8

Marzachí C, Bosco D (2005) Relative Quantification of Chrysanthemum Yellows (16Sr I) Phytoplasma in Its Plant and Insect Host Using Real-Time Polymerase Chain Reaction. Molecular Biotechnology 30: 117-127

Mori N, Pavan F, Bondavalli R, Reggiani N, Paltrinieri S, Bertaccini A (2008) Factors affecting the spread of "Bois Noir" disease in north Italy vineyards. Vitis 47:65-72

Musetti R, Marabottini R, Badiani M, Martini M, Sanitá di Toppi L, Borselli S, Borgo M, Osler R (2007) On the role of H2O2 in the recovery of grapevine (Vitis vinifera cv. Prosecco) from Flavescence dorée disease. Functional Plant Biology 34: 750-758

Namba S, Kato S, Iwanami S, Oyaizu H, Shiozawa H, Tsuchizuki T (1993) Detection and differentiation of plant-pathogenic mycoplasmalike organisms using polymerase chain reaction. Phytopathology 83: 786-791

Nielson MW (1979) Taxonomic relationships of leafhopper vectors of plant pathogens. Leafhoppers Vectors and Plant Disease Agents (Maramorosch K, Harris KF eds) pp. 2-27. Academic Press, New York

Osler R, Carraro L, Loi N, Refatti E (1993) Symptom expression and disease occurrence of a yellows disease of grapevine in northeastern Italy. Plant Disease 77: 496-498

Osler R, Loi N, Refatti E (1995) Present knowledge on phytoplasma disease of fruit trees and grapevine. 2nd Slovenian Conference on Plant Protection in Radenci: 27-46

Riedle-Bauer M, Hanak K, Regner F, Tiefenbrunner W (2010) Influence of pruning measures on recovery of Bois Noir-infected grapevines. Journal of Phytopathology 158:628-632

Saracco P, Marzachi C, Bosco D (2008) Activity of some insecticides in preventing transmission of chrysanthemum yellows phytoplasma ('Candidatus Phytoplasma asteris') by the leafhopper Macrosteles quadripunctulatus Kirschbaum. Crop Protection 27:130-136

SA Wine Industry Statistics nr 37 (2013) SA Wine Industry Information & Systems, SAWIS, PO Box 238, Paarl 7620.

Seemüller E, Schneider B, Maurer R, Ahrens U, Daire X, Kison H, Lorenz KH, Firrao G, Avinent L, Sears B, Stackebrand E (1994) Phylogenetic classification of phytopathogenic

Mollicutes by sequence analysis of 16S Ribosomal DNA. International Journal of Systematic Bacteriology 44 (3): 440-446

Seemüller E, Marcone C, Lauer U, Ragozzino A, Goschl M (1998) Current status of molecular classification of the phytoplasmas. Journal of Plant Pathology 80: 3-26

Spinas N (2012) The efficacy of the antimicrobial peptides D4E1, VvAMP-1 and Snakin1 against the grapevine pathogen aster yellows phytoplasma. MSc Thesis. Stellenbosch University

Strauss E (2009) Phytoplasma Research Begins to Bloom. Science 325: 388-390

Terlizzi F, Credi R (2007) Uneven distribution of stolbur phytoplasma in Italian grapevines as revealed by nested-PCR. Bulletin of Insectology 60 (2): 365-366

Uyemoto JK, Bethell RE, Kirkpatrick BC, Brown KW, Munkvold GP, Marois JJ (1998) Eradication as a control measure for X-disease in California cherry orchards. Acta Horticulturae 472:715–721

Weintraub PG, Beanland L (2006) Insect vectors of phytoplasmas. Annual Review of Entomology 51:91–111

Weintraub PG, Jones P (2010) Phytoplasmas: Genomes, Plants Hosts and Vectors. CABI

Weisburg WG, Tully JG, Rose DL, Petzel JP, Oyaizu H, Yang D, Mandelco L, Sechrest J, Lawrence TG, Van Etten J (1989) A phylogenetic analysis of the mycoplasmas: basis for their classification. J Bacteriol 171 6455–6467

Woese CR (1987) Bacterial evolution. Microbiology Review. 51:221-271

Chapter 3
Sensitivity of a nested PCR versus Real-Time PCR in phytoplasma detection

3.1. Introduction

Since the original identification of phytoplasmas, scientists have struggled to accurately diagnose infection in plants due to the inability to culture the organism *in vitro*. Methods used to detect phytoplasmas include biological, serological and nucleic acid-based techniques.

In the past, identification of phytoplasma infection was based on the observation of characteristic symptoms in infected plants, plant host range, relationships with insect vectors and in a few cases, plants treated with the antibiotic tetracycline, resulting in the disappearance of symptoms which further supported a phytoplasma diagnosis (Lee *et al*, 2000). Subsequently, the microscopic examination of ultra-thin cuttings of infected phloem tissue was used to diagnose diseases of possible phytoplasma origin (Lee *et al*, 2000). Researchers applied electron microscopy as well as graft transmission to healthy plants in order to catalogue phytoplasmas (Bertaccini and Duduk, 2009). DNA-binding fluorescent dyes such as 4',6-diamidino-2-phenylindole (DAPI) were commonly used in laboratories and was accurate when phytoplasma numbers were high, although low infections presented inconsistent results (Seemüller and Kirkpatrick, 2006). These methods, used to gain insight into phytoplasma diagnosis, became futile when the need to distinguish different phytoplasmas arose. Biological methods also were determined to be labour intensive and unreliable, thus the need for a robust and precise technique rendered itself vital.

In the 1980s, researchers focused on the development of serological assays that could possibly provide an accurate phytoplasma diagnosis. This lead to the production of poly- and monoclonal antibodies, which were used to detect Flavescence dorée (Belli *et al*, 2010) and observe phytoplasmas by immunosorbent electron microscopy (ISEM) and fluorescent light microscopy (Lherminier *et al,* 1989). Enzyme-linked immunosorbent assay was also a common diagnostic tool used in laboratories (Lee *et al*, 2000). Serological assays, however limited, proved to be simple and reliable. Limitations arose when researchers needed to

distinguish different phytoplasmas from each other (Lee *et al*, 2000). This disadvantage together with the difficulty of antisera production caused the phasing out of these techniques.

The breakthrough in phytoplasma diagnostics emerged when the first DNA probes based on phytoplasma sequences were produced and subsequently the development of recombinant DNA techniques (Kirkpatrick *et al*, 1987). DNA hybridization successfully detected phytoplasma in periwinkle (*Catharanthus roseus*) and other herbaceous plants; however, results were inconsistent when applied to woody plants, and in particular, grapevines. This was attributed to the pathogen's low titer and irregular distribution in the plant (Belli *et al*, 2010). The significant achievement in molecular assays detecting phytoplasmas in plants and insect hosts arose with the diagnosis using Polymerase Chain Reaction (PCR). This was made possible by the accessibility of the 16S rRNA gene sequences of Aster Yellows, Bois Noir and Flavescence dorée related phytoplasmas in the NCBI database (Lim and Sears, 1989; Davis *et al*, 1993; Daire *et al*, 1993). These sequences allowed the design of universal primers for PCR assays which are able to detect all known phytoplasmas in the plants hosts and insect vectors, increasing its popularity. The technique was further developed into the ability to detect phytoplasma subgroups using Restriction Fragment Length Polymorphism (RFLP) and Nested PCR (Lee *et al,* 1994; Bianco *et al,* 1996). Detection by PCR requires isolation of good quality DNA with high phytoplasma titer, which has proven difficult when working with woody plants such as grapevines. Total DNA extracted from infected plants will have less than 1% of phytoplasma DNA and has been shown to contain plant polyphenolics and polysaccharides known to inhibit enzymes in PCR (Bertaccini, 2007). Nested PCR is the preferred method of detection. This is due to the preliminary amplification step allowing the technique to be undeterred by low titers and PCR inhibitors (Gunderson *et al*, 1994). However, the analysis is time consuming and false positives have proven to be a substantial risk as samples undergo a procedure comprised of multiple steps (Angelini *et al*, 2007).

In recent years, Real-Time or quantitative PCR (qPCR) techniques have been applied for phytoplasma detection. TaqMan® and SYBR green reactions have been used for diagnosis of several subgroups of phytoplasmas. However, problems arose when these specific assays cross reacted with phytoplasmas from other subgroups (Hodgetts *et al*, 2009). Christensen *et al* (2004) demonstrated a TaqMan® assay that had the ability to amplify all 16Sr subgroups except 16SrIV, 16SrXIII and 16SrXIV. This was established for universal diagnosis of phytoplasmas in plants, yet in grapevines, there are few robust and reliable qPCR protocols

for phytoplasma detection and most of those require a preliminary conventional PCR step, thereby eliminating the ability to quantify (Bianco *et al*, 2004). In 2007, Angelini *et al* developed a novel TaqMan qPCR assay for detecting phytoplasmas associated with grapevine yellows. Primers and probes were designed based on the 16S rRNA genes, with further research showing the abundance of false positives. These false positives were proven to be the amplification of various unculturable bacteria (Hodgetts *et al*, 2009). A new universal and multiplex qPCR assay was developed using primers and probes based on the 23S rRNA genes. This multiplex PCR had the ability to detect phytoplasmas from all groups and simultaneously amplifying DNA from phytoplasmas in group 16SrI (Hodgetts *et al*, 2009).

There are two approaches to quantify genes in Real-Time PCR, namely absolute quantification and relative quantification. Relative quantification depends on the comparison of the expression levels between the target gene and a housekeeping gene which acts as a reference. This strategy is usually sufficient for studying the physiological changes that occur with gene expression levels. Absolute quantification requires the construction of a standard/calibration curve. This curve, as well as the previously calculated copy per reaction numbers, is used to extrapolate values of unknown samples. This approach is usually used for determining viral copy numbers (http://strategy.gene-quantification.info/).

There have been few direct comparisons between nested PCR and Real-Time PCR with regards to detecting low titers of phytoplasma infection. As grapevines are woody plants, phytoplasma titers can be very low and thus difficult to diagnose. The aim of this research chapter was to determine whether nested PCR, Real-Time PCR with a TaqMan probe or Real-Time PCR with a melt curve analysis is the most reliable, accurate and sensitive assay for phytoplasma detection and ultimately which of these techniques will be used for further research in this study.

3.2. Materials and Methods

3.2.1 Sample Collection and DNA Extraction

Samples were collected in the Vredendal area of the Western Cape, South Africa. The collection of samples included grapevines previously identified as being infected with phytoplasma and those grapevines that presented typical Aster Yellows phytoplasma symptoms. A total of 30 samples were collected in January 2013. These samples were used

for protocol optimization and experiments aimed at determining the temporal distribution of the pathogen.

The DNA was extracted from *V. vinifera* cv Chardonnay, previously determined to be infected with Aster Yellows phytoplasma, using the NucleoSpin® Plant II kit (Macherey-Nagel). Quality and concentration of DNA was determined using the Nanodrop® ND-1000 spectrophotometer.

3.2.1. Nested PCR

A positive sample previously diagnosed and obtained from Vredendal, South Africa was diluted to 10 ng/µL using MilliQ water. Healthy plant DNA (10 ng/µL) was used to further dilute the DNA from positively infected samples. Thus the final concentrations of the phytoplasma infected DNA used for the nested PCR were 1 ng/µL, 0.1 ng/µL, 0.01 ng/µL, 0.001 ng/µL, $0.1x10^{-3}$ ng/µL, and $0.1x10^{-4}$ ng/µL. This dilution series was used to test the sensitivity of the nested PCR assay.

Primers used for the nested PCR are shown in Table 3.1.

Table 3.1: Primers used in the Nested PCR protocol

Primer	Sequence	Position	Amplicon size	Reference
P1	5'-AAG AGT TTG ATC CTG GCT CAG GAT T-3'	16S rDNA	1792 bp	Deng *et al*, 1991
P7	5'-CGT CCT TCA TCG GCT CTT-3'	23S rDNA		Schneider *et al*, 1995
R16F2n	5'-GAA ACG ACT GCT AAG ACT GG-3'	16S rDNA	1244 bp	Gunderson *et al*, 1996
R16R2	5'-TGA CGG GCG GTG TGT ACA AAC CCC G-3'	16S rDNA		Lee *et al*, 1993
R16(I)F1	5'-TAA AAG ACC TAG CAA TAG G-3'	16S rDNA	1 100 bp	Lee *et al*, 1994
R16(I)R1	5'-CAA TCC GAA CTG AGA CTG T-3'	16S rDNA		Lee *et al*, 1994

The 20 µL reaction mixtures contained 1µl of extracted DNA (10-50ng), 0.2 µM of each primer, 10 mM of dNTP mix (Thermo Scientific), 1X KapaTaq Buffer B with Mg, 1X cresol and 0.9U/µL KapaTaq DNA polymerase. The PCR conditions for the first PCR with primers P1 and P7 started with an initial denaturation step of 94 °C for 5 minutes, followed by 35

cycles of 20 seconds of denaturation at 94 °C, 30 seconds of primer annealing at 55 °C and 45 seconds of extension at 72 °C. The final extension step was 7 minutes at 72 °C. The products obtained by direct amplification were diluted 1:10 with sterile DEPC water and used in the first nested PCR with primers R16F2n and R16R2. The second nested PCR used primers R16(I)F1 and R16(1)R1 for further amplification with the products of R16F2n and R16R2 diluted at 1:10. The conditions for both nested PCR assays began with the initial denaturation at 94 °C for 2 minutes, followed by 35 cycles of the denaturation step for 1 minute at 94 °C, primer annealing for 2 minutes at 58 °C for the first nested PCR and 50 °C for the second and extension for 3 minutes at 72 °C. The final extension step was 10 minutes at 72 °C.

Final PCR products were analyzed by electrophoresis through a 1% agarose gel with ethidium bromide and visualization using a UV transilluminator.

3.2.2. Real-Time PCR

A Rotor-Gene Q (Qiagen) thermal cycler was used to perform the Real-Time PCRs and the Rotor-Gene Q Series Software 1.7 was used for setting up the runs and analysing results. Two different RT-PCR protocols were tested, both following the absolute quantification strategy. The first protocol used Syto9 as a dye, without a commercial master mix, and a post run melt curve was performed. The second protocol used a TaqMan probe and the Illuminaris Color Probe qPCR Master Mix.

3.2.2.1 Real-Time PCR with Melt Curve analysis

For construction of the standard curve, primers in table 3.2 were used to amplify a sequence from the 16S rDNA genes. Primers were designed by Visser (2011) and were based on those originally designed by Angelini *et al* (2007) and Hollingsworth *et al* (2008).

Table 3.2: Primers used for the Real-Time PCR with a melt curve analysis

Primer	Sequence	Position	Reference
AY-F	5'- AAA CCT CAC CAG GTC TTG -3'	16S rDNA genes	Hollingsworth *et al,* 2008
AY-R	5'- AAG TCC CCA CCA TTA CGT -3'	16S rDNA genes	Angelini *et al,* 2007

Amplicons were excised from the gel following electrophoresis and purified using the Zymoclean kit and cloned into the PGEM-T Easy cloning vector. The plasmid was termed pAY2. A 7-fold dilution series (1ng to 1fg) was established by diluting pAY2 in 20 ng/µL of total DNA from a healthy *V. vinifera* cv Chardonnay plant. The number of template copies per reaction was calculated to be $1.14x10^{8}$ (http://cels.uri.edu/gsc/cndna.html). Each dilution was performed in triplicate and Rotor-Gene Q Series Software 1.7 automatically calculated the threshold levels, threshold cycles and standard curves.

Each 20 µL reaction used for the standard curve and sample analysis contained 1X Kapa Buffer B with Mg+, 0.2 µM of each primer, 0.25 µM dNTPs, 1.25 µM Syto9 dye, 1U KapaTaq and 1 µL of sample DNA diluted to 20 ng/µL with MilliQ water. The cycling conditions were as follows; 5 minute denaturation step at 95 °C, 35 cycles of denaturation for 10 seconds at 95 °C, annealing of primers for 15 seconds at 60 °C and extension for 15 seconds at 72 °C and lastly the final extension step for 5 minutes at 72 °C. After amplification, a melt curve analysis was performed from 70 °C to 95 °C in order to determine the specificity of the PCR products.

To determine the sensitivity of the assay, the same dilution series used for the nested PCR was utilized. Healthy plant DNA at a concentration of 10 ng/µL was spiked with DNA from Aster Yellows phytoplasma infected plants. The final concentrations of the dilutions were 10 ng/µL, 1 ng/µL, 0.1 ng/µL, 0.01 ng/µL, 0.001 ng/µL, $0.1x10^{-3}$ ng/µL, and $0.1x10^{-4}$ ng/µL.

3.2.2.2 Real-Time PCR with a TaqMan probe

A sequence from the 23S rDNA genes was amplified using the primers shown in Table 3.3 and the fragment was excised from the gel using the Zymoclean™ Gel DNA Recovery Kit following electrophoresis. The band was cloned into the cloning vector, PGEM-T Easy (Promega) and was termed pAY3. For the construction of the standard curve, a 7-fold dilution series (1ng to 1fg) was established by diluting pAY3 in 20ng/µl of total DNA from a healthy *V. vinifera* cv Chardonnay plant. The calculated template copy number per reaction using 1ng of pAY3 was $2.97x10^{8}$. This was calculated using an online calculator for determining the number of copies of a template (http://cels.uri.edu/gsc/cndna.html). All reactions were performed in triplicate for each pAY3 dilution. Rotor-Gene Q Series Software 1.7 automatically calculated the threshold levels, threshold cycles and standard curves.

Table 3.3: Primers and probes used for absolute quantification of Aster Yellows phytoplasma

Primer	Sequence	Position	Reference
JH-F1	5'-GGT CTC CGA ATG GGA AAA CC -3'	23S rDNA genes	Hodgetts *et al*, 2009
JH-R	5'-CTC GTC ACT ACC RGA ATC GTT ATT AC-3'	23S rDNA genes	Hodgetts *et al*, 2009
JH-P1	6-FAM- CGC GGC GAA CTG AAA T-MGB	23S rDNA genes	Hodgetts *et al*, 2009

To determine the reliability of the reaction, a multiplex PCR was designed using primers and probe which amplifies a sequence from the *cytochrome c oxidase* (*COX*) gene found in the mitochondrial DNA of plants. The *COX* gene has been successfully used as an endogenous control (Hodgetts *et al* (2009)), allowing the researcher to distinguish a failed reaction due to PCR inhibitors and not mistake it for a negative result. The probe used for detection of Aster Yellows phytoplasma was designed with the FAM reporter and MGB quencher and florescence is seen in the green/HRM channels. The Luminaris Color Probe qPCR Master Mix (Thermo Scientific) was used with the recommended reaction setup. A final volume of 20 µL per reaction was used, which included 10 µL of the 2X Master Mix, 0.6 µL of each primer at 10 µM, 0.4 µL of each probe also at 10 µM, 2.5 µL of template DNA and nuclease free water. A dilution series was prepared from 10 ng – 1 fg in 10 ng/µL of plant DNA previously tested negative for phytoplasma infection. The thermal cycling was performed using a two-step cycling protocol recommended. This started with the UDG pre-treatment at 50°C for 2 minutes, followed by the initial denaturation at 95°C for ten minutes. Afterwards, 40 cycles of a 15 second denaturation step at 95°C and a 60 second annealing and extension step at 60°C were performed. Data acquisition was executed during the annealing/extension step. Florescence from amplification of the Aster Yellows phytoplasma fragment was visualized in the Green channel whereas the amplification of the cytochrome oxidase fragment was visualized in the Yellow channel. Results were analyzed using the average cycle threshold (C_T) values and absolute quantification was achieved by comparison with the dilution series of the pAY3 plasmid.

The identical dilutions series previously used was analyzed in order to determine sensitivity and directly compare the two previous assays.

3.3. Results

3.3.1 Nested PCR

In total, three PCRs were performed and analyzed by electrophoresis. No amplicons were present in Figure 3.1. In the first nested PCR two amplicons are visible (Figure 3.2). Lane 2 in Figure 3.2 contained the undiluted sample at a concentration of approximately 1300 ng/µL. No visible band was observed. The bands present in lanes 3 and 4 correspond to the dilutions of 10 ng/µL and 1 ng/µL, respectively. The second set of primers were successful at amplifying phytoplasma but are unable to do so at lower concentrations. After the second nested PCR using the third and final set of primes, Aster Yellows phytoplasma detected can be seen up to the third last dilution (0.0001 ng/µL) as seen in Figure 3.3. Using the previous nested PCR products as template DNA results in enough target sequences for sufficient amplification thus allowing observation of an amplicon through gel electrophoresis.

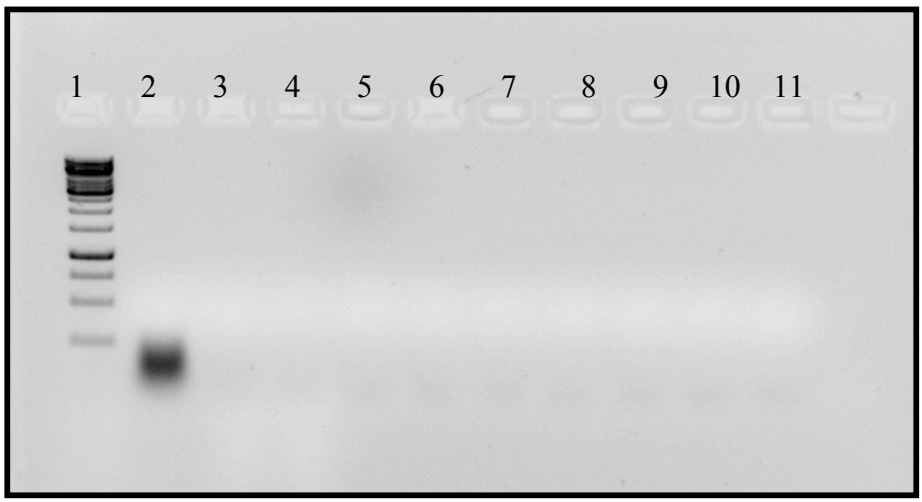

Figure 3.1: Agarose gel electrophoresis of PCR products using primers P1/P7. No amplicons can be seen due to insufficient amplification. Lane 1: 1Kb molecular marker. Lane 2: Undiluted DNA of a positive control. Lane 3: DNA of positive control diluted to 10 ng/ul. Lane 4-10: Tenfold dilution of 1 ng/ul-0.000001ng/ul. Lane 11: No template control.

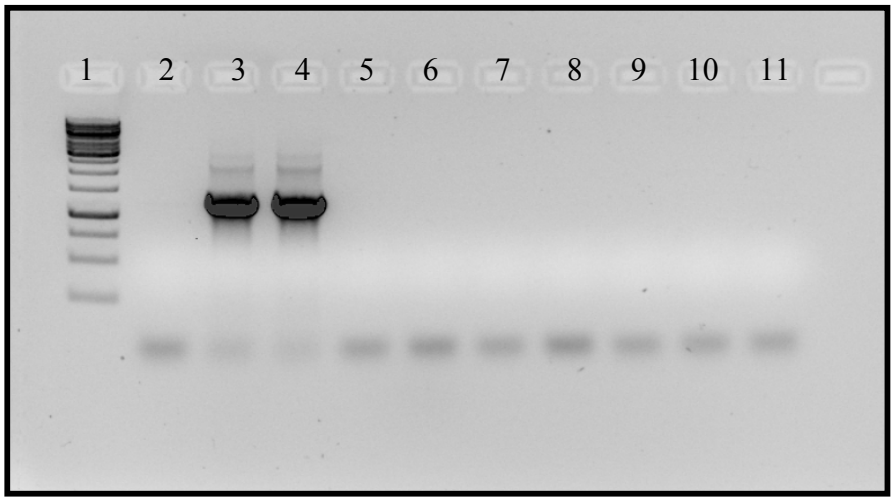

Figure 3.2: Agarose gel electrophoresis of products of PCR using primers R16F2n/ R16R2. Amplicons can be seen in lanes 3 and 4. Lane 1: 1Kb molecular marker. Lane 2: Undiluted DNA of a positive control. Lane 3: DNA of positive control diluted to 10ng/ul. Lane 4-10: Tenfold dilution of 1ng/ul-0.00001ng/ul. Lane 11: No template control.

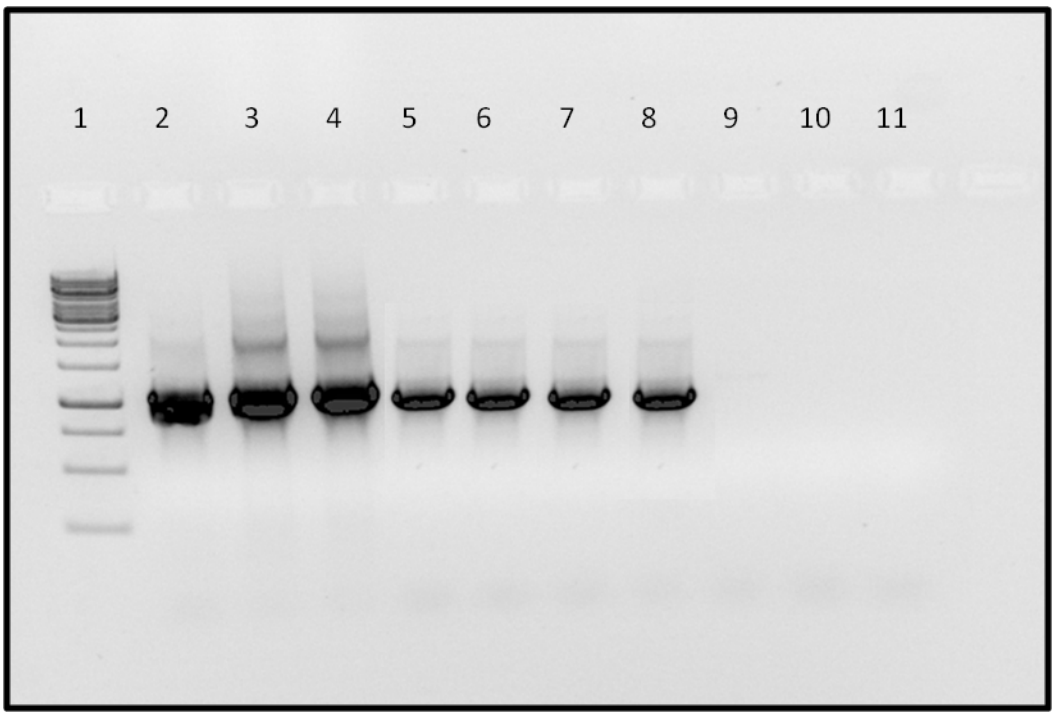

Figure 3.3: Agarose gel electrophoresis of products of PCR using primers R16(I)F1/R16(I)R1. Amplicons can be seen in lanes 2-8 representing Aster Yellows phytoplasma. Lane 1: 1Kb molecular marker. Lane 2: Undiluted DNA of a positive control. Lane 3: DNA of positive control diluted to 10ng/ul. Lane 4-10: Tenfold dilution of 1ng/ul-0.00001ng/ul. Lane 11: No template control.

3.3.2 Real-Time PCR

3.3.2.1 Real-Time PCR with melt curve analysis

The standard curve was constructed by plotting the mean C_T value of each standard dilution against the logarithm of their concentrations. The efficiency of this standard curve was calculated to be 0.98. The slope (M value) was -3.38, and the regression correlation efficient (R^2) was 0.99904 (Table 3.4).

Table 3.4: Quantitation information of standard curve for Real-Time PCR with melt curve analysis

Standard Curve (1)	conc= 10^(-0.296*C_T + 11.861)
Standard Curve (2)	C_T = -3.380*log(conc) + 40.089
Reaction efficiency (*)	(* = 10^(-1/m) - 1) 0.97639
M	-3.37984
B	40.08903
R Value	0.99952
R^2 Value	0.99904

Table 3.5 shows the results of the standard curve along with figure. Dilutions up to and including $1x10^{-5}$ ng/µL, showed florescence before cycle 30. Figure shows the melt curve performed after the reactions were complete. All samples showed a melting peak at 87 ºC.

Table 3.5: C_T values and calculated concentrations of each dilution in the standard curve

Colour	Dilution (ng/µL)	C_T	Given Conc (copies/reaction)	Calc Conc (copies/reaction)
	1	12.60	1.14E+08	1.17E+08
	1	12.62	1.14E+08	1.15E+08
	1	12.74	1.14E+08	1.06E+08

Colour	Dilution (ng/µL)	C_T	Given Conc (copies/reaction)	Calc Conc (copies/reaction)
	0.1	15.84	1.14E+07	1.28E+07
	0.1	15.82	1.14E+07	1.29E+07
	0.1	15.85	1.14E+07	1.27E+07
	0.01	19.25	1.14E+06	1.25E+06
	0.01	19.48	1.14E+06	1.07E+06
	0.01	19.38	1.14E+06	1.15E+06
	$1x10^{-3}$	23.01	1.14E+05	9.63E+04
	$1x10^{-3}$	23.09	1.14E+05	9.13E+04
	$1x10^{-3}$	22.97	1.14E+05	9.93E+04
	$1x10^{-4}$	26.29	1.14E+04	1.03E+04
	$1x10^{-4}$	26.32	1.14E+04	1.01E+04
	$1x10^{-4}$	26.18	1.14E+04	1.11E+04
	$1x10^{-5}$	29.31	1.14E+03	1.31E+03
	$1x10^{-5}$	29.13	1.14E+03	1.48E+03
	$1x10^{-5}$	29.47	1.14E+03	1.18E+03
	$1x10^{-6}$			
	$1x10^{-6}$			
	$1x10^{-6}$			
	0			
	0			
	0			

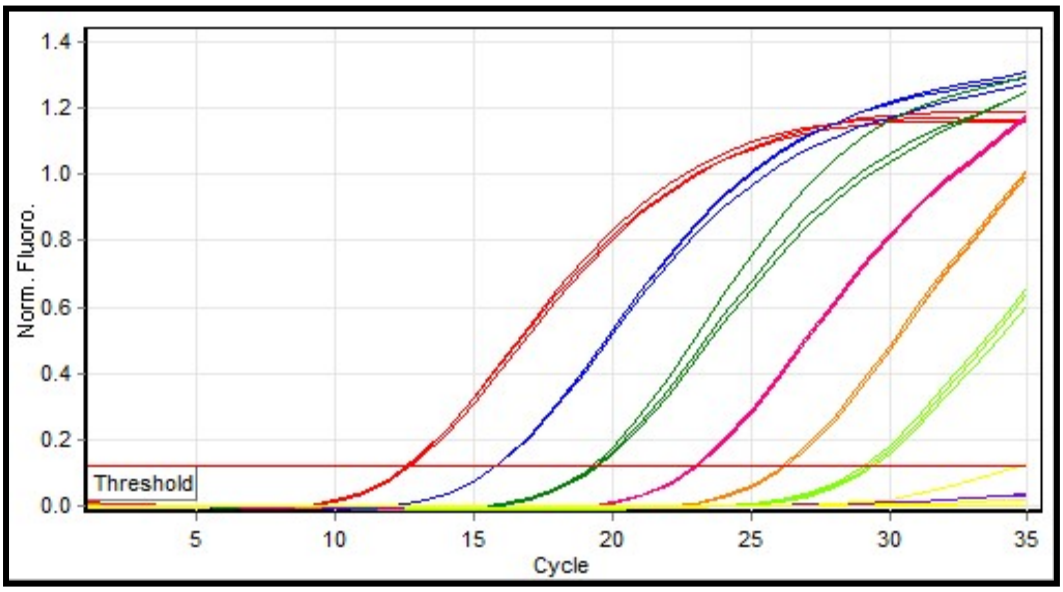

Figure 3.4: Amplification profile of the dilution series used to construct the standard curve for the Real-Time PCR using Syto9. See Table 3.5 for colour key.

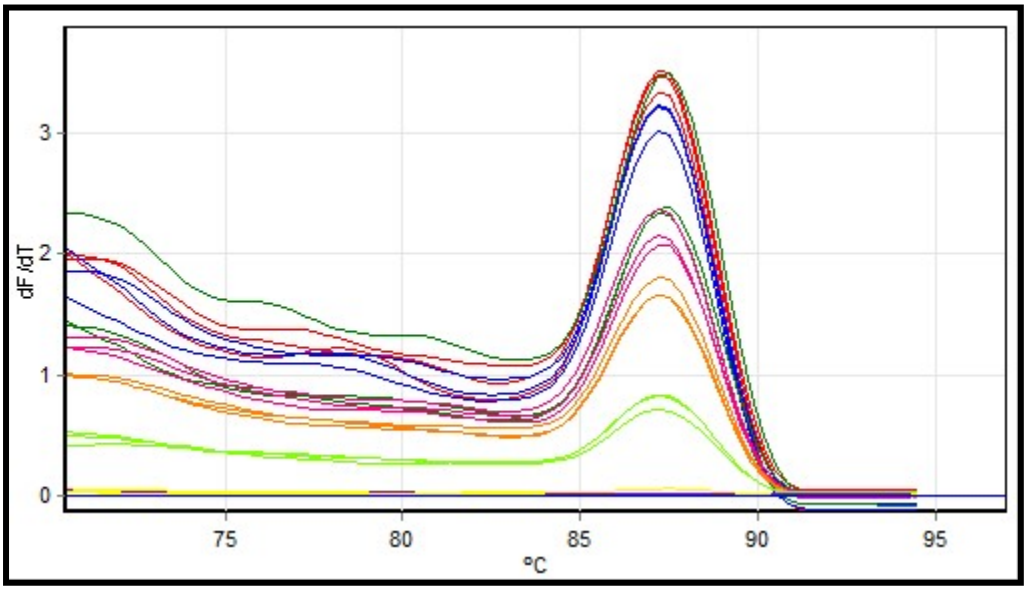

Figure 3.5: Melt curve analysis of the standard curve. All curves peak at 87 ^{o}C. See Table 3.5 for colour key.

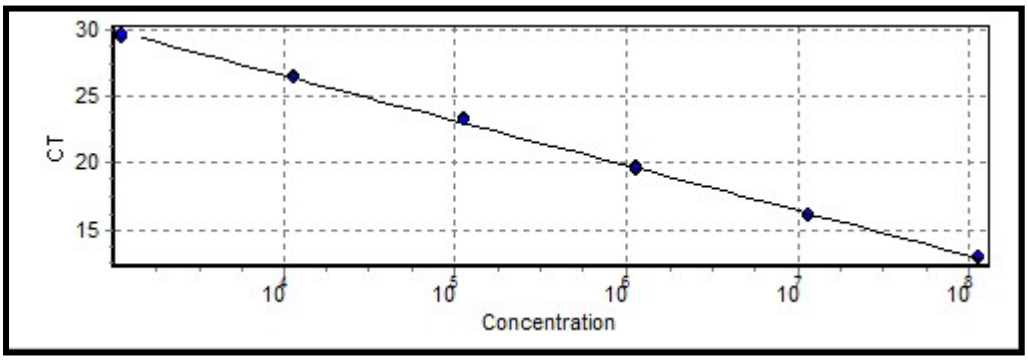

Figure 3.6: Standard curve calculated by the software by using the C_T values of each triplicate and plotting the values against the final concentrations of each sample.

After the construction of the standard curve, the dilution series used for the nested PCR was tested with this Real-Time PCR assay in order to compare sensitivity.

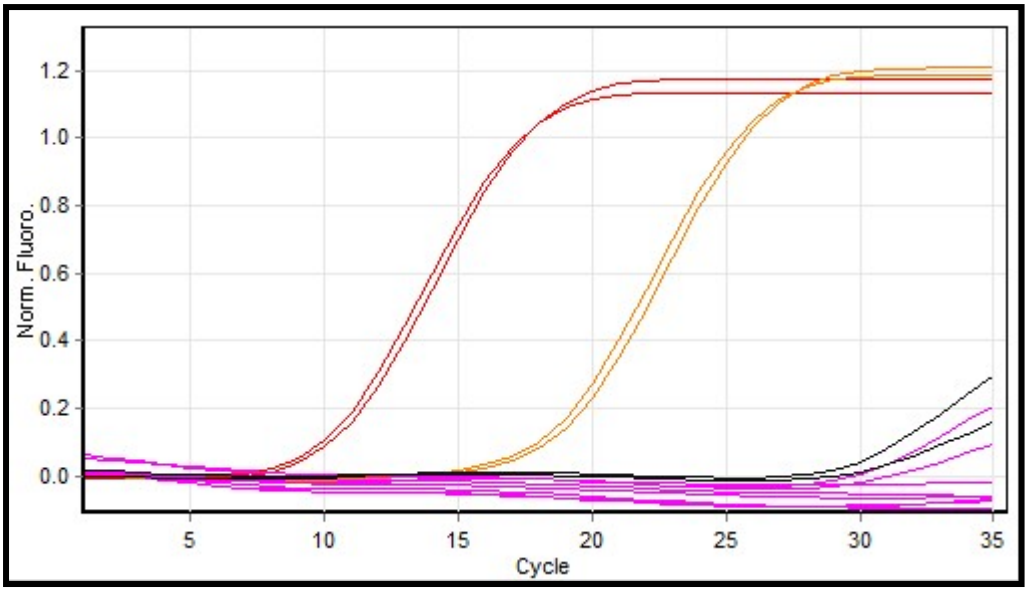

Figure 3.7: Amplification profile of the dilution series used to test assay sensitivity for the Real-Time PCR with Syto9. Red represents the plasmid control, orange represents the positive plant control, pink represents the unknown samples and black represents the no template control.

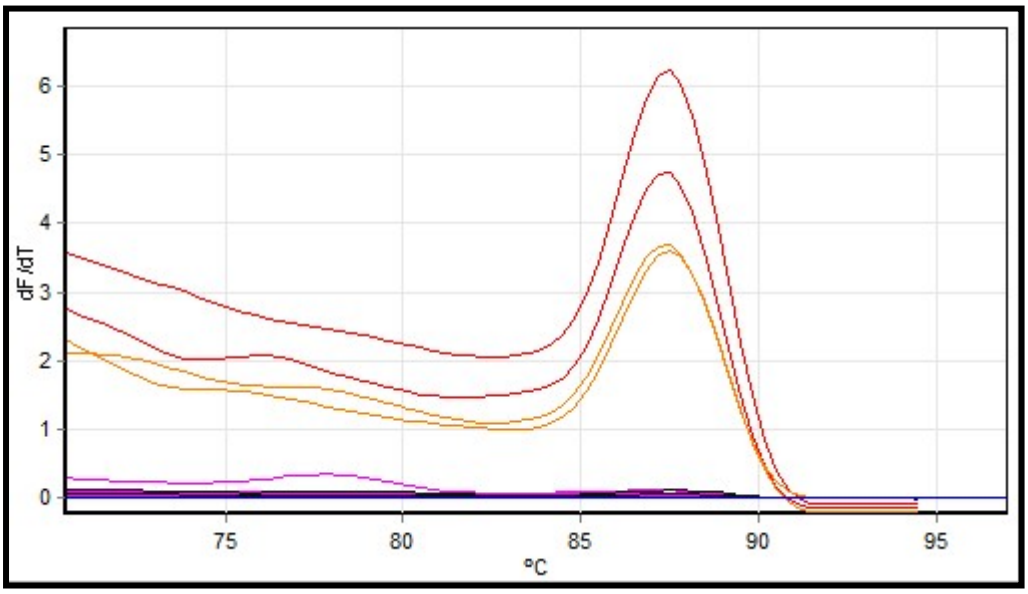

Figure 3.8: Melt curve analysis of the dilution series used to test assay sensitivity of the Real-Time PCR with Syto9. Curves peak at 87 °C. Red represents the plasmid control, orange represents the positive plant control, pink represents the unknown samples and black represents the no template control.

3.3.2.2 Real-Time PCR with TaqMan Probe

The standard curve was constructed by plotting the mean C_T value of each standard dilution against the logarithm of their concentrations. The dilution factor was 1:10. The efficiency of this standard curve was calculated to be 1.00. The slope (M value) was -3.32, and the regression correlation efficient (R2) was 0.9987 (Table 3.6). These values allow the standard curve to be used for accurate quantification in further analyses.

Table 3.6: Quantitation information of standard curve for Real-Time PCR with a TaqMan probe

Threshold	0.0485
Standard Curve (1)	conc= 10^(-0.301*CT + 11.970)
Standard Curve (2)	CT = -3.321*log(conc) + 39.749
Reaction efficiency (*)	(* = 10^(-1/m) - 1) 1.0005
M	-3.32073
B	39.74913
R Value	0.99938
R^2 Value	0.99877

Table 3.7: Ct values and calculated concentrations of each dilution in the standard curve

Colour	Dilution (ng/µL)	Ct	Given Conc (copies/reaction)	Calc Conc (copies/reaction)
	1	11.51	2.97E+08	3.19E+08
	1	11.54	2.97E+08	3.12E+08
	1	11.53	2.97E+08	3.15E+08
	0.1	14.53	2.97E+07	3.92E+07
	0.1	14.87	2.97E+07	3.10E+07
	0.1	14.82	2.97E+07	3.21E+07
	0.01	18.14	2.97E+06	3.21E+06
	0.01	18.72	2.97E+06	2.15E+06
	0.01	18.32	2.97E+06	2.84E+06

Colour	Dilution (ng/µL)	Ct	Given Conc (copies/reaction)	Calc Conc (copies/reaction)
	$1x10^{-3}$	21.60	2.97E+05	2.91E+05
	$1x10^{-3}$	21.97	2.97E+05	2.26E+05
	$1x10^{-3}$	21.65	2.97E+05	2.81E+05
	$1x10^{-4}$	25.14	2.97E+04	2.51E+04
	$1x10^{-4}$	25.11	2.97E+04	2.57E+04
	$1x10^{-4}$	25.02	2.97E+04	2.72E+04
	$1x10^{-5}$	28.24	2.97E+03	2.93E+03
	$1x10^{-5}$	28.24	2.97E+03	2.91E+03
	$1x10^{-5}$	28.25	2.97E+03	2.91E+03
	$1x10^{-6}$	31.69	2.79E+02	2.67E+02
	$1x10^{-6}$	31.00	2.79E+02	4.32E+02
	$1x10^{-6}$	31.45	2.79E+02	3.15E+02
	0			
	0			

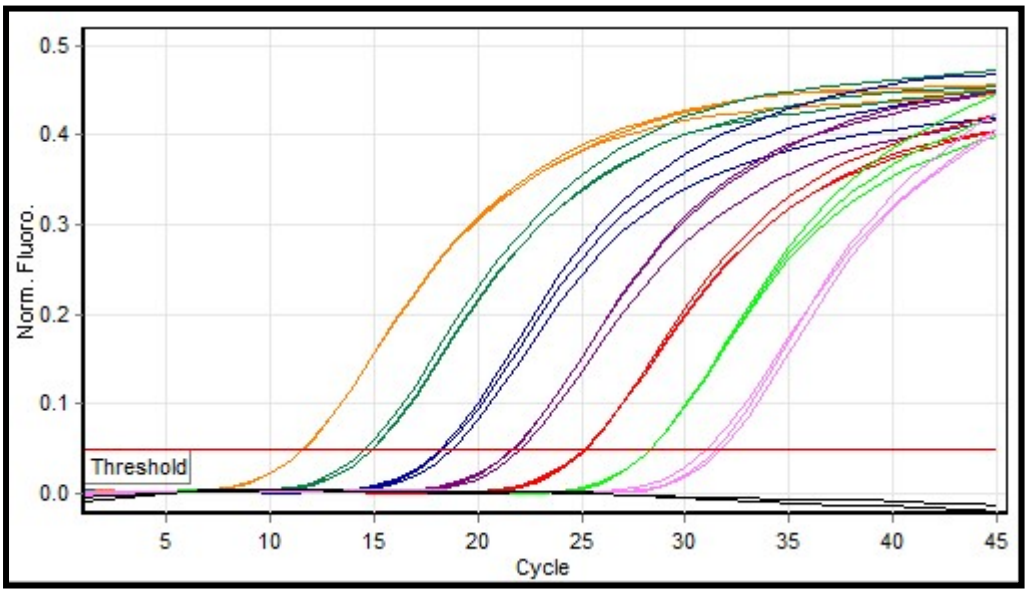

Figure 3.9: Amplification profile of the dilution series used to construct the standard curve for the Real-Time PCR with a TaqMan probe. See table 3.7 for colour key.

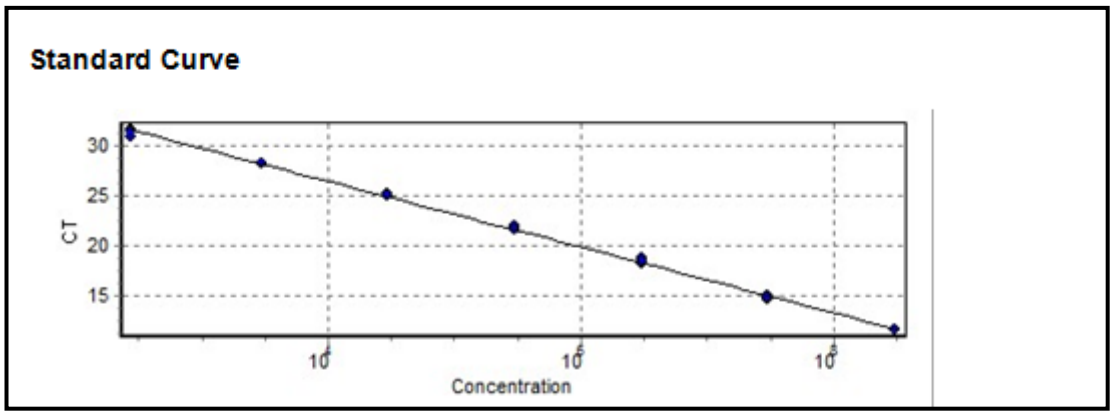

Figure 3.10: The standard curve resulting from the CT values of each triplicate plotted against the concentrations of each sample.

Once the standard curve had been constructed the dilution series used for the nested PCR was used in the Real-Time PCR. The results can be seen in the amplification profile below (Figure 3.11).

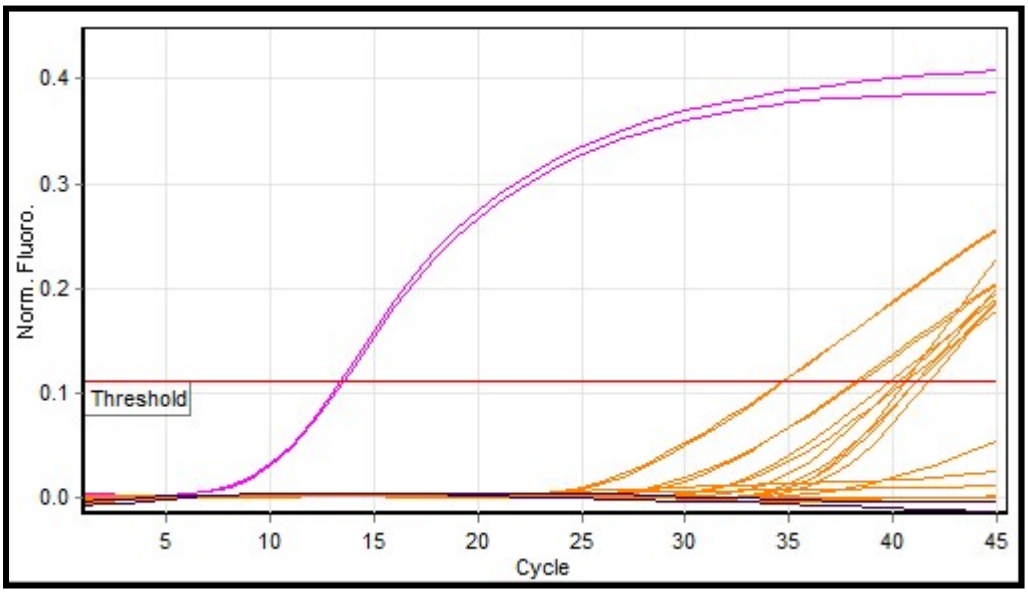

Figure 3.11: Amplification profile of the dilution series testing assay sensitivity for the Real-Time PCR with a TaqMan probe. The pink represents the plasmid control, orange represents unknowns and black represents the no template control.

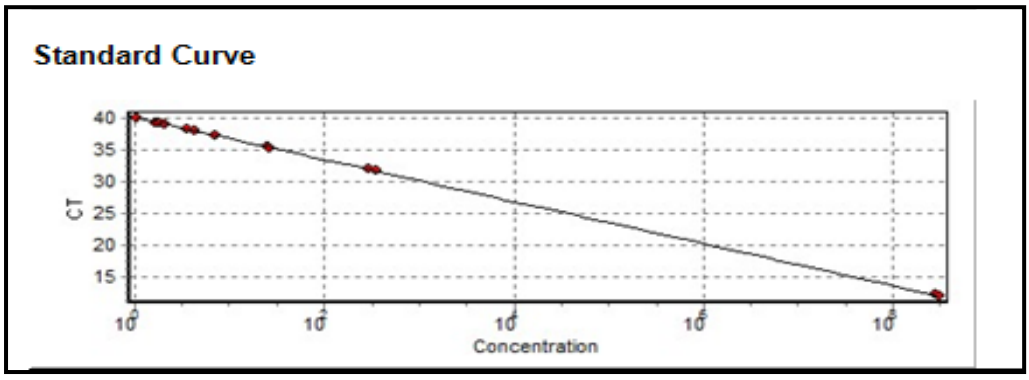

Figure 3.12: The standard curve resulting from the CT values of each duplicate plotted against the concentrations of each sample for the Real-Time PCR with a TaqMan probe.

The samples that showed florescence after cycle 35 were unreliable. This may have been due to contamination and were classified as negative for infection. Florescence was observed up until the dilution 0.1 ng/µL. This would be problematic if samples taken for further research had low infection titers and results would be unreliable. It would be difficult to make the distinction between a true positive infection that has a low titer of phytoplasma and a negative result.

Table 3.8 compares the results of the three assays and shows that the nested PCR is the most sensitive assay as it detected Aster Yellows phytoplasma up until the 0.0001 ng/µL dilution.

Table 3.8: A comparison of PCR sensitivity between the Nested PCR protocol and the Real-Time PCR protocol by using a dilution series

DNA Concentration	Nested PCR	Real-Time PCR with melt curve analysis	Real-Time PCR with TaqMan Probe
Undiluted	✓		✓
10	✓	✓	✓
1	✓		✓
0.1	✓		
0.01	✓		
0.001	✓		
0.0001	✓		
0.00001			
0.000001			

3.4 Discussion and Conclusion

There has been a considerable amount of research directed at designing a perfect assay with which to detect phytoplasmas. In grapevine this has proven to be more difficult as phytoplasma tends to have a low titer and has a very erratic distribution within the plant. The aim of this project was to determine the spatial and temporal distribution of Aster Yellows phytoplasma in grapevine, thus making it paramount that a reliable, robust and sensitive assay be used.

Nested PCR with primers P1/P7 and R16F2n/R16R2 are universal phytoplasma diagnostic primers and have been used to diagnose phytoplasma infection in a wide variety of plant and insect hosts (Gunderson and Lee, 1994). The second set of primers is designed to anneal to a region within the product amplified with the first set of primers. This is said to increase the sensitivity 100 fold (Gunderson and Lee, 1994). The third pair of primers, R16(I)F1/R16(I)R1, amplify a sequence smaller than that of the second pair, found within the second amplicon (See figure 3.13). This substantially increases sensitivity.

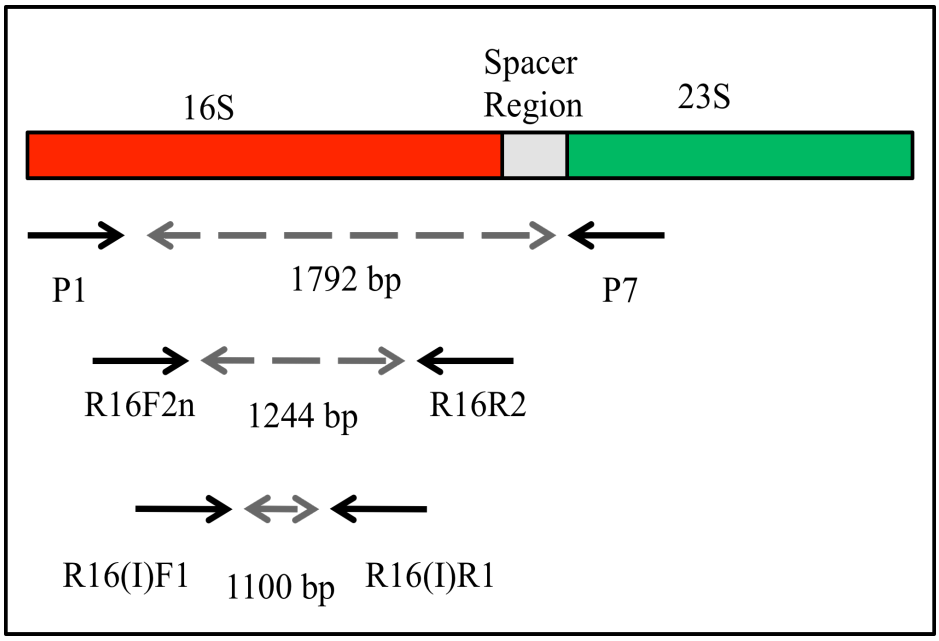

Figure 3.13: Illustration depicting the positions of the three primer pairs required for Nested PCR. This figure is not to scale.

Figure 3.1 shows no amplification using primers P1/P7. Concentration of PCR products could be too low to be visualised on a gel due to the low titer of phytoplasma infection in the sample. In Figure 3.2, the first lane shows no amplification, however this is the undiluted DNA sample and lack of amplification could be due to the higher quantity of PCR inhibitors in the template DNA or that the PCR reagents were exhausted before the product was sufficiently amplified. Ultimately, this verifies the necessity of diluting the template DNA to a more workable concentration. DNA samples used for further amplification in both the nested PCR and Real-Time PCR assays were diluted thus lowering the possible presence of inhibitors. Figure 3.3 shows the results of the second nested PCR with primers R16(I)F1/R16(I)R1. Lane 2 represents the undiluted DNA sample which was at a concentration of approximately 60 ng/µL. The amplicon can only be visualized after this set of primers were used thus proving amplification is only possible once possible PCR inhibitors are diluted. Lane 2 shows the sample of DNA diluted to 10 ng/µL with MilliQ water. The proceeding dilutions (lanes 4-10) were diluted with 10 ng/µl of healthy plant DNA. This was done in order to get an accurate understanding of the sensitivity of the PCR when diagnosing samples with very low titers of Aster Yellows phytoplasma infection. Amplicons can be visualized until the dilution 0.0001 ng/µL.

Real-Time PCR was initially the assay of choice due to the ability to quantify. The sensitivity of two Real-Time PCR protocols was tested. The first assay used was one that required a melt

curve analysis after completion of amplification. This assay used Syto9, a double stranded DNA specific dye, and primers designed by Visser (2011) and were based on those originally designed by Angelini *et al* (2007) and Hollingsworth *et al* (2008). These primers amplified a fragment from the 16S rDNA genes of phytoplasma. The standard curve was sufficient to use for quantification. For a standard curve to be acceptable for quantification purposes, the efficiency should be between 90-110%, guaranteeing doubling of the amplicon at each cycle. For the current assay the efficiency was 98%. The efficiency is calculated using the following formula: $E = 10^{(-1/slope)} - 1$. The slope value was generated by the software, and should be between -3.3 to -3.6. In table 3.4, one can see the M value or slope was calculated to be -3.38.

The sensitivity of this Real-Time PCR was then evaluated by using the same dilution series compiled for the nested PCR in order to have a direct comparison. Amplification was evident for only the plasmid standard and the DNA sample diluted to 10 ng/µL. There was no fluorescence for the remaining samples (Figure 3.7). This assay showed low sensitivity and was thus not optimal for further experiments.

Primers designed by Hodgetts *et al* (2009) were used for the second Real-Time PCR assay as these provided a diagnostic able to determine whether phytoplasma is present in group 16SrI or in another group. These primers were accompanied by a probe allowing accurate detection. TaqMan probe assays have a higher specificity than assays with a dsDNA binding dye. Preliminary testing of known positive controls proved that the primers and probe were successfully amplifying Aster Yellows phytoplasma. This allowed the construction of the plasmid pAY3 and subsequently the standard curve. This standard curve showed an efficiency of 100% allowing it to be sufficient for quantification.

The assay was also used to test its sensitivity by amplification of the dilution series of both previous assays. Figure 3.11 displays the amplification plot showing florescence for the undiluted sample, the sample at 10 ng/µL and the further dilutions of phytoplasma positive DNA up until 1 ng/µL. Thus the TaqMan probe assay proved to be more sensitive than the Syto9 Real-Time PCR.

Table 3.8 shows the comparison of all three assays using the same dilution series of the DNA extracted from a plant infected with Aster Yellows phytoplasma. Nested PCR is the most sensitive as it detected phytoplasma up to the dilution, 0.0001 ng/µL. Real-Time PCR is known to be more sensitive and reliable of the PCR assays, however it depends on the type of chemistry used in the assay. SYBR ® Green Syto9 chemistry tends to be less specific than

the use of TaqMan ® Probes as they can reduce the possibility of amplifying non-specific target DNA. This was validated, as the comparison between the two assays showed that the Real-Time PCR with a TaqMan probe is more sensitive.

Comparisons between the nested PCR and Real-Time PCR assays have been done in the past, however the nested PCR was only tested with the first two primer pairs. Hren *et al* (2007) designed a TaqMan probe assay for detecting Flavescence doreé (FD) and Bois Noir and subsequently compared it to the universal nested PCR. Their results can be seen in figure 3.14. It was shown that the Real-Time PCR was more sensitive than the nested when testing FD. However, only two primer pairs were used for the nested PCR in the study, as opposed to the three pairs used in this chapter. There have been no comparisons between the Real-Time PCR assay with primers designed by Hodgetts *et al* (2009) and the three step nested PCR. Evaluation of the sensitivity in this chapter showed that the nested PCR with three primer pairs and two nested PCR steps is more sensitive than that of both Real-Time PCR assays.

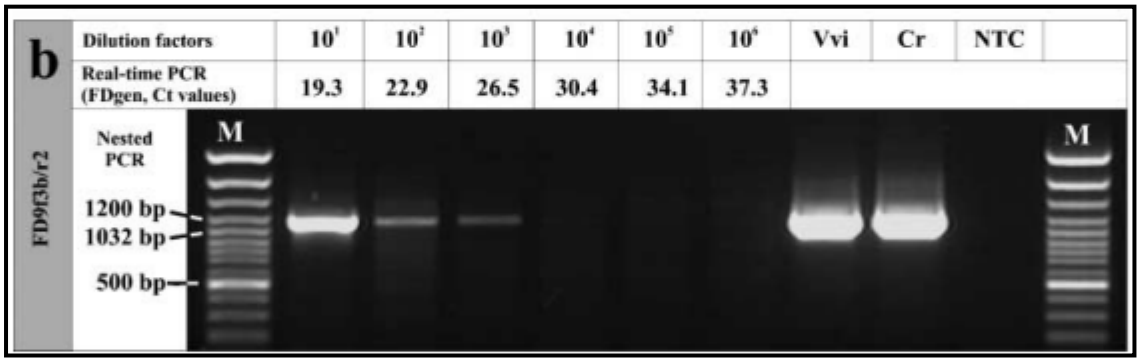

Figure 3.14: Results of a comparison between nested PCR and Real-Time PCR for Florescence doreé detection done by Hren *et al* (2007).

Should samples collected for the further research chapters in this study have low infection titers then the nested PCR would be the optimal assay to use. The assay proved to be reproducible and reliable.

3.5. References

Angelini E, Bianchi GN, Filippin L, Morassutti C, Borgo M (2007) A new TaqMan method for the identification of phytoplasmas associated with grapevine yellows by real-time PCR assay. Journal of Microbiological Methods 68:613-622

Belli G, Bianco PA, Conti M (2010) Grapevine yellows in Italy: Past, Present and Future. Journal of Plant Pathology 92 (2): 303-326

Bertaccini A (2007) Phytoplasmas: diversity, taxonomy, and epidemiology. Frontiers in Bioscience 12, 673-689

Bertaccini A and Duduk B (2009) Phytoplasmas and phytoplasma diseases: a review of recent research. Phytopathologia Mediterranea 48: 355-378

Bianco PA, Casati P, Marziliano N (2004) Detection of phytoplasmas associated with grapevine Flavescence dorée disease using real-time PCR. Journal of Plant Pathology. 86, 259-264

Bianco PA, Davis RE, Casati P, Fortusini A (1996) Prevalence of aster yellows (AY) and elm yellows (EY) group phytoplasmas in symptomatic grapevines in three areas of northern Italy. Vitis 4: 195-199

Daire X, Clair D, Reinert W, Boudon-Padieu E (1997) Detection and differentiation of Grapevine yellows phytoplasmas belonging to the elm yellows and to the Stolbur subgroup by PCR amplification of non-ribosomal DNA. European Journal of Plant Pathology 103: 507-514

Davis RE, Dally EL, Bertaccini A, Lee I-M, Credi R (1993) Restriction fragment length polymorphism analyses and dot hybridization distiguish mycoplasmalike organisms associated with flavescence dorée and southern European grapevine yellows disease in Italy. Phytopathology 83: 772-776

Deng S, Hiruki C (1991) Amplification of 16S rRNA genes from culturable and nonculturable mollicutes. Journal of Microbiological Methods 14:53-61

Gundersen DE, Lee I-M (1996) Ultrasensitive detection of phytoplasmas by nested-PCR assays using two universal primer pairs. Phytopathologia Mediterranea 35:144-151

Gunderson DE, Lee I-M, Rehner SA, Davis RE, Kingbury DT (1994) Phylogeny of mycoplasmalike organisms (phytoplasmas): a basis for their classification. Journal of Bacteriology 176: 5244-5254

Hodgetts J, Boonham N, Mumford R, Dickinson M (2009) Panel of 23S rRNA gene-based Real-Time PCR assays for improved universal ad group-specific detection of phytoplasmas. Applied and Environmental Microbiology 75 (9): 2945-2950

Hren M, Boben J, Rotter A, Kralj P, Gruden K, Ravnikar M (2007) Real-time PCR detection systems for Flavescence dorée and Bois noir phytoplasmas in grapevine: comparison with conventional PCR detection and application in diagnostics. Plant Pathology 56:785-796

Kirkpatrick BC, Stenger DC, Morris TJ, Purcell H (1987) Cloning and detection of DNA from a nonculturable plant pathogenic mycoplasma-like organism. Science 238: 197- 200

Lee I-M, Gundersen DE, Hammond RW, Davis RE (1994) Use of mycoplasmalike organism (MLO) group specific oligonucleotide primers for nested-PCR assays to detect mixed-MLO infections in a single host plant. Phytopathology 84: 559-566

Lee I-M, Davis RE, Gundersen-Rindal DE (2000) Phytoplasma: phytopathogenic mollicutes. Annual Review of Microbiology 54:221-255

Lim PO and Sears BB (1989) 16S rRNA sequence shows that plant-pathogenic “mycoplasmalike organisms” are evolutionarily distinct from animal mycoplasmas. Journal of Bacteriology 171: 5901-5906

Lherminier J, Terwisscha Van Scheltinga T, Boudon-Padieu E, Caudwell A (1989) Rapid immunfluorescent detection of the grapevine Flavescence dorée mycoplasma-like organism in the salivary glands of the leafhopper *Euscelidius variegatus* KBM. Journal of Phytopathology 125: 353-360

Schneider B, Cousin M-T, Klinkong S, Seemüller E (1995) Taxonomic relatedness and phylogenetic positions of phytoplasmas associated with disease of faba bean, sunnhemp, sesame, soybean, and eggplant. Zeitschrift fuer Pflanzenkrankheiten und Pflanzenschutz 102:225-232

Seemüller E and Kirkpatrick BC (1996) Detection of phytoplasma infections in plants. *In* Tully JG, Razin S. (eds), Molecular and diagnostic procedures in mycoplasmology, Academic Press, Inc., San Diego, California. p 299-311

Visser M (2011) An evaluation of the efficacy of antimicrobial peptides against grapevine pathogens. MSc thesis. Department of Genetics, Stellenbosch University

Internet Sources

http://strategy.gene-quantification.info/

http://cels.uri.edu/gsc/cndna.html

Chapter 4
Spatial Distribution of Aster Yellows phytoplasma in grapevine

4.1. Introduction

Diagnosing Aster Yellows phytoplasma in plants has proven difficult for scientists and farmers alike, especially when studies involve grapevine plants. Diagnosis is a vital component contributing to further understanding of the plant pathogen and ultimately discovering ways in which to control it. Issues that arise when detecting the phytoplasma include the change of titer of the pathogen over time and the spatial distribution within the plant.

A spatial distribution of phytoplasmas was suggested when asymptomatic plant material was diagnosed with phytoplasma infection (Gibb *et al*, 1999; Constable *et al*, 2003). This provides evidence that symptom expression is not an indication of where in the plant the phytoplasma is most abundant. There have also been cases where symptomatic material did not present positive results when using molecular detection techniques (Carstens, 2014). When attempting to diagnose phytoplasma infections in crops all around the world, it is generally accepted that leaves and petioles displaying strong symptoms, such as the yellowing colours, are collected. Samples displaying these symptoms can yield negative results, providing evidence of a definite spatial distribution making accurate detection very difficult.

Christensen and associates recorded in 2004 that phytoplasma was unevenly distributed in the plants *C. roseus* and *E. pulcherrima*. It was found that there were no phytoplasmas present in any of the sink tissues. Titer levels were low in root samples, higher in stem samples and the highest titers were found in the petiole samples of the plants. Terlizzi and Credi (2007) performed a study using nested PCR where leaf, shoot, dormant cane and cordon samples were tested for stolbur phytoplasma. The preliminary results obtained suggested uneven distribution within the plant. It was stated that stolbur rarely spreads throughout the grapevine in a systemic pattern. This was verified by the low percentage of Bois Noir transmission when grafting cuttings from infected grapevines. Their final findings concluded that leaf

material presented the best sample type for accurate diagnosis as Stolbur phytoplasma was detected in all leaf samples collected (Terlizzi and Credi, 2007).

A preliminary study on the spatial distribution of Aster Yellows phytoplasma was performed on 5 canes (cv. Chardonnay) collected from Vredendal, South Africa. DNA from the phloem and leaf samples was extracted and tested using nested PCR. It was found that 61% of the node material yielded positive results where as only 31% of leaf samples collected from the canes were infected. Figure 4.1 shows the 5 canes and where the Aster Yellows phytoplasma was detected. There were several cases where the leaf sample presented positive results while its corresponding node did not. However, 90% of the leaf samples that yielded positive results corresponded with positive results obtained in the node samples (Spinas, 2012). Spatial distribution is not well understood due to the lack of research available regarding the mechanism of phytoplasmas in plant hosts.

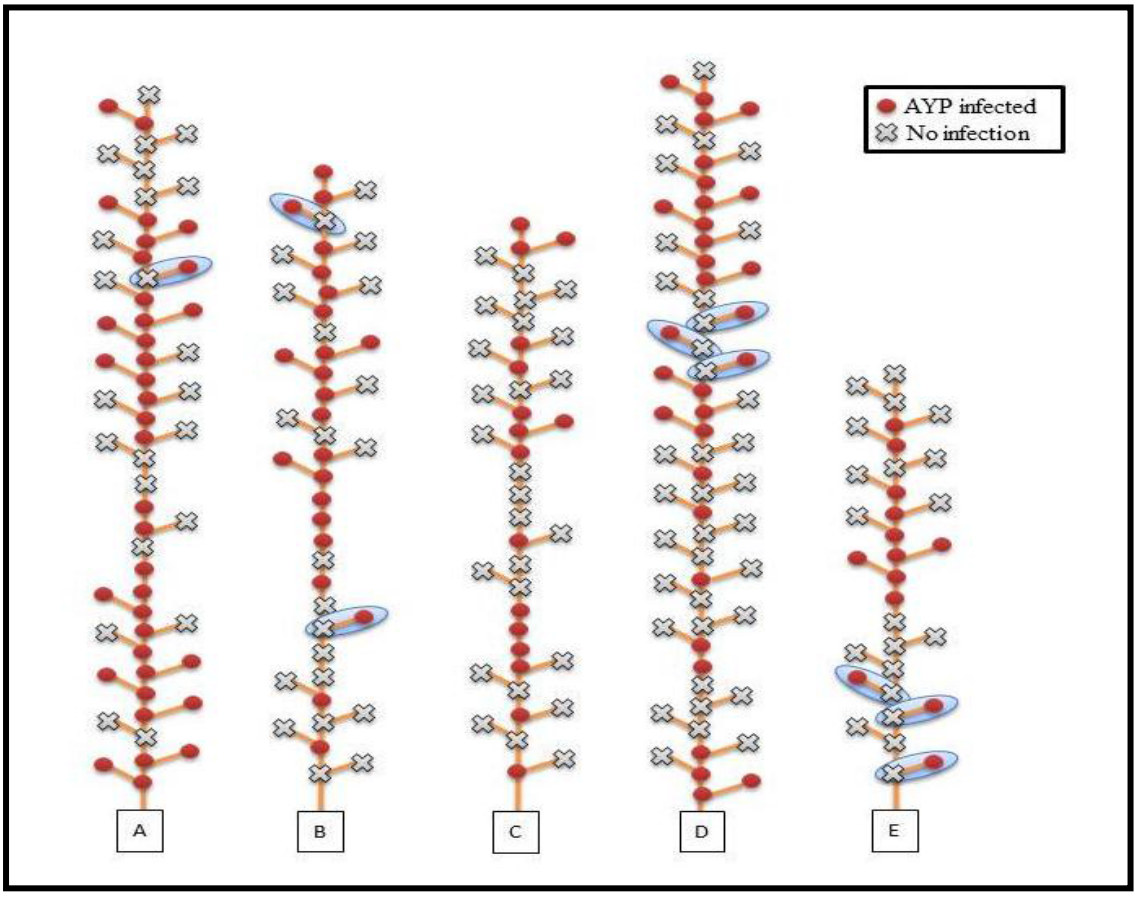

Figure 4.1: Depiction of the 5 canes and the location of detected Aster Yellows phytoplasma infection. The red spots show positive results whereas the white crosses show negative results. The blue circles depict instances where the leaf sample was positive for the phytoplasma and the corresponding node did not (Adapted from Spinas, 2012).

Phenological stages may have an effect on the distribution of phytoplasmas. A study was performed by Del Serrone *et al* (1996) on the effects that six different phenological stages may have on detection of phytoplasmas. The highest titers of phytoplasmas were found during the berry-ripening stage in leaf tissue extracts. Phytoplasma was also found in the phloem extracted from cane samples during this stage (Del Serrone *et al*, 1996). These conclusions contribute to the hypothesis that multiple plant tissues contain phytoplasmas and can be used for detection.

There are no definite results that clearly demonstrate which plant tissues (in particular grapevine) should be utilized for accurate detection. The aim of this research was to determine which part of a grapevine plant yields the most positive results and can be further used for accurate detection of Aster Yellows phytoplasma in vineyards.

4.2 Methods and Materials

4.2.1 Sample Collection

Samples were collected from Vredendal, South Africa. In April 2013, seven grapevine plants cv. Chenin Blanc, that presented noticeable Aster Yellows phytoplasma symptoms were sampled. Leaf and petiole samples were transported in dry ice once flash frozen in liquid nitrogen for further experimentation.

In October 2013, three of the seven whole grapevine plants were removed from the vineyard. For transport, canes were removed from the trunks and the trunks were sawn into fragments. The roots were pulled out of the ground and separated according to size. Figure 4.2 shows plant 7 being removed from the vineyard.

Sample types collected were; leaves with their corresponding petioles, canes, trunks and roots.

Figure 4.2: (A) Photograph of plant 7 prior to extraction from the ground. (B) Photograph of plant 7 in the process of fragmenting the trunk following cane removal. (C) Photograph of the site from which plant 7 was removed.

4.2.2 Sample Preparation and DNA Extraction

The seven leaf and petiole samples collected in April 2013 were macerated using liquid nitrogen in a mortar and pestle until a fine powder resulted. The Nucleospin Plant II DNA Extraction kit was used with 0.1 g of ground material. Quality of the DNA was determined by gel electrophoresis and Nanodrop.

Preparation of the 3 whole-plant samples were as follows; leaf and petioles were removed from canes and phloem scrapings were collected from the canes and trunks. Roots were washed to remove soil and soil organisms. Table 4.1 shows a list of the samples collected and prepared from each of the three plants. All samples were macerated using liquid nitrogen in a mortar and pestle. 0.1 g of the fine ground material was used in the Nucleospin Plant II DNA Extraction kit. Quality of the DNA was determined by gel electrophoresis and concentration was measured by a Nanodrop® ND-1000 spectrophotometer.

Table 4.1: List of samples collected from each of the 3 grapevine plants

Sample Type	Plant 1	Plant 2	Plant 3
Leaf	20	13	8
Petiole	8	4	6
Cane Scrapings	12	7	6
Trunk Scrapings	9	7	0
Small Root	2	5	4
Medium Root	5	3	0
Large Root (phloem scrapings)	5	4	3

4.2.3 Diagnostics

Nested PCR and Real-Time PCR were used to detect Aster Yellows phytoplasma in the 7 samples collected in April 2013. See protocols in sections 3.2.1 and 3.2.2.2, respectively.

The Real-Time PCR assay failed to detect phytoplasma in any of the 131 samples collected in October 2013. Thus a nested PCR was used. See protocol in section 3.2.1.

PCR products were analyzed by electrophoresis through a 1% agarose gel with ethidium bromide and visualized with a UV transilluminator.

4.2.4 Sequence Validation

Several amplicons were excised from the 1 % gel and purified using Zymoclean™ Gel DNA Recovery Kit. The excised amplicons were sequenced using Sanger Sequencing and subsequently analyzed using nucleotide BLAST.

4.3 Results

4.3.1 DNA Extraction

Total DNA extracted from all types of samples yielded concentrations ranging from 20 ng/µL to 40 ng/µL. In order to ensure consistency, all samples were diluted to 20 ng/µL with MilliQ water.

4.3.2 Diagnostics

Both nested PCR and Real-Time PCR were used to detect Aster Yellows phytoplasma in the 7 samples collected in April 2013. Figure 4.3 shows the final results of the nested PCR and figure 4.4 shows the amplification profile obtained from the Real-Time PCR. The nested PCR showed 4 out of the 7 samples collected to be positive for Aster Yellows phytoplasma infection.

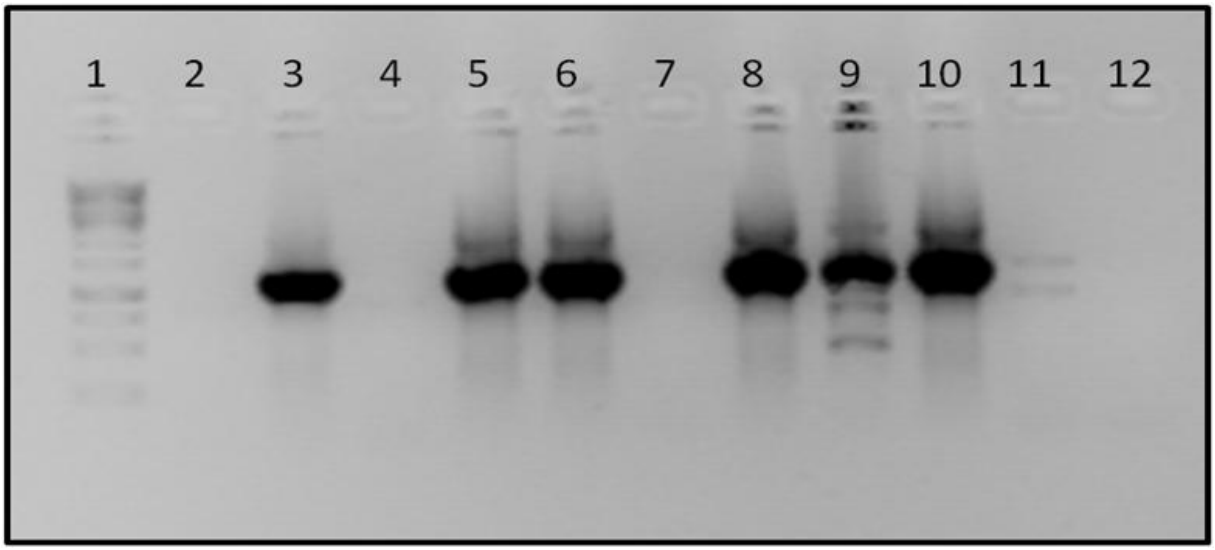

Figure 4.3: Agarose gel showing the products of the nested PCR. Lane 1 is a 1 kb marker. Lane 2-8 are the unknown samples collected in April 2013. Plants 2, 4, 5 and 7 are seen in lanes 3, 5, 6 and 7 respectively. Lane 9 and 10 are positive controls. Lane 11 is the negative control. Lane 12 is the no template control.

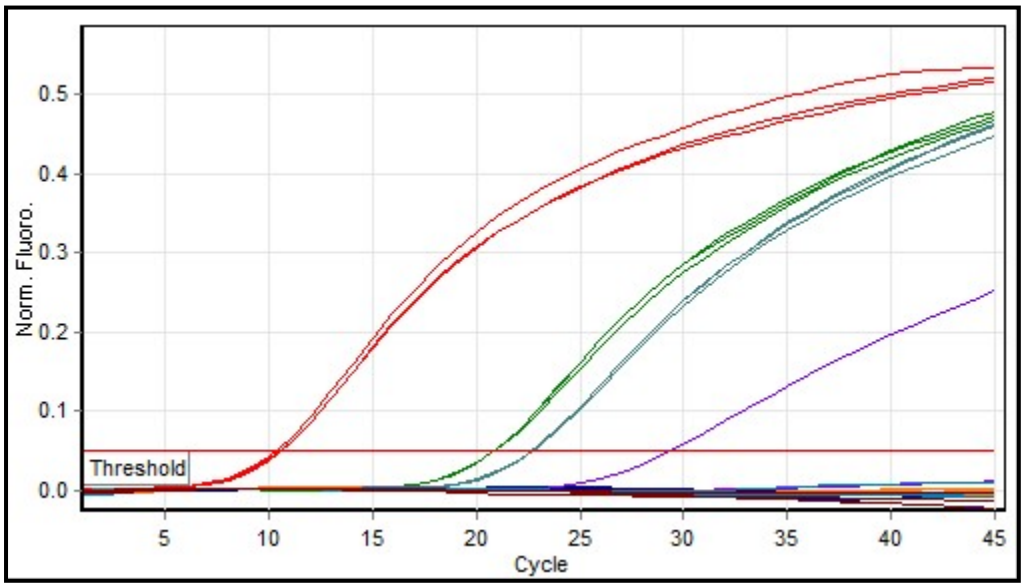

Figure 4.4: Amplification profile of the Real-Time PCR showing florescence for the standard and 2 out of the 7 samples collected. Red represents the plasmid control, green represents plant 7, blue represents plant 4, purple represents plant 2, orange represents plant 1, navy represents plant 3, orange represents plant 5, brown represents plant 6 and black represents no template control.

Plants 2, 4, 5 and 7 yielded positive results when using the nested PCR protocol, but only plants 4 and 7 appeared to be positive when diagnosed using the Real-Time PCR protocol. Plants 2, 4 and 7 were chosen for further experimentation.

4.3.3 Spatial Distribution

Following DNA extraction and dilution, an initial diagnosis was performed on 18 samples using the Real-Time PCR protocol. Figure 4.5 shows the amplification profile of the results obtained. Fluorescence was only observed on the standard and the positive control.

The same samples were utilized in the nested PCR protocol and results can be seen in Figure 4.6. Out of the 15 samples tested, 5 yielded positive results. The nested PCR was then chosen for further analysis of remaining samples.

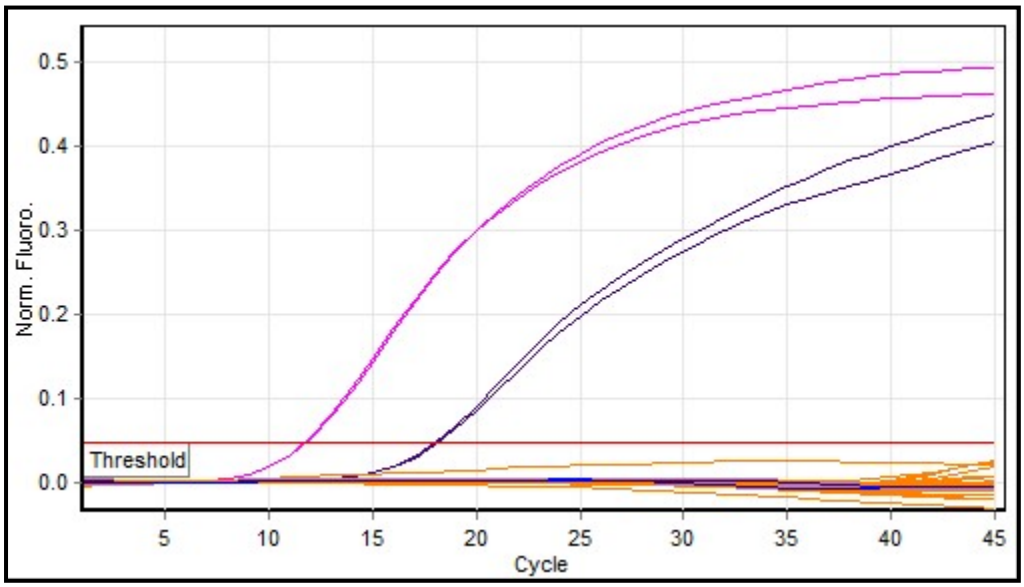

Figure 4.5: Amplification profile of the initial diagnosis of 18 random samples. Pink represents the plasmid control, navy represents the positive control, orange represents the 18 unknown samples and blue represents the no template control.

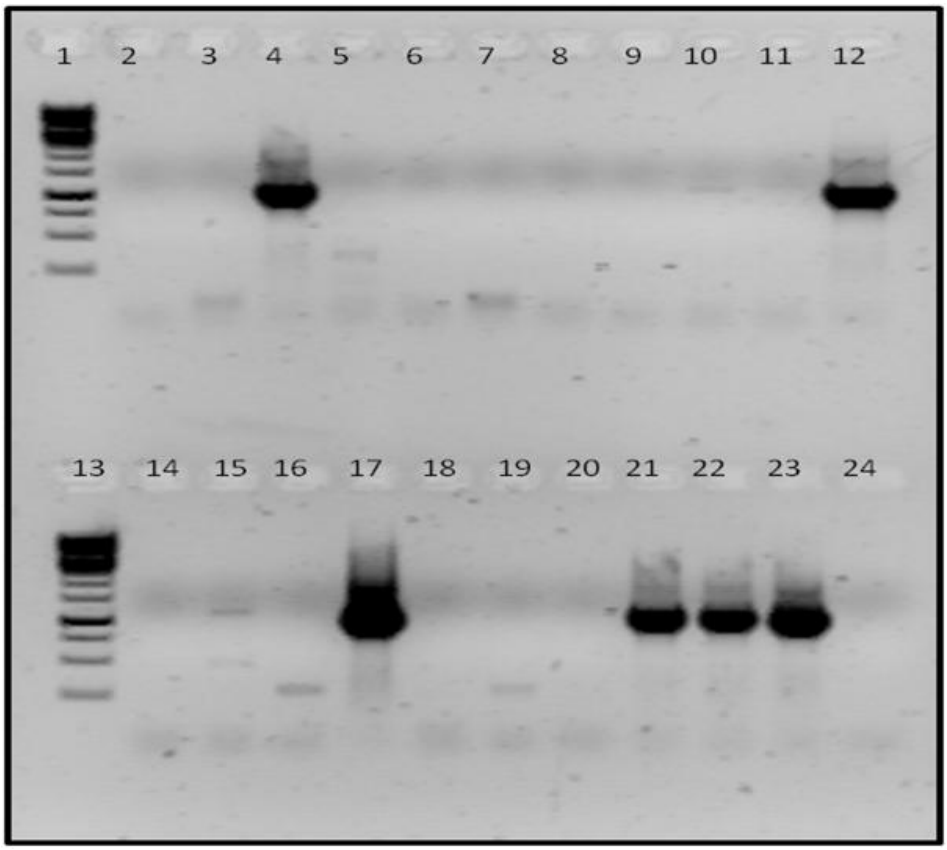

Figure 4.6: Agarose gel showing products of the initial nested PCR testing 18 random samples. Lane 1 and 13 are 1 kb markers. Lane 2 and 3 are negative controls. Lanes 4-12, and 14-22 are the unknowns. Lane 23 is the positive control and lane 24 is the no template control.

The results of the analyses of the remaining samples can be seen in tables 4.2-4.5.

Table 4.2: Results of the analyses performed on plant 7

Sample Type	Number of Positive samples	Total Samples Collected	Percentage of Positive samples out of total number of sample type	Total Percentage of positive samples out of total samples collected
Trunk	2	9	22%	3%
Cane	4	12	33%	7%
Petiole	1	8	13%	2%
Leaf	4	20	20%	7%
Root	0	12	0%	0%
Total	11	61	18%	

Table 4.3 Results of the analyses performed on plant 4

Sample Type	Number of Positive samples	Total Samples Collected	Percentage of Positive samples out of total number of sample type	Total Percentage of positive samples out of total samples collected
Trunk	3	7	43%	7%
Cane	3	7	43%	7%
Petiole	0	4	0%	0%
Leaf	2	13	15%	5%
Root	2	12	17%	5%
Total	10	43	23%	

Table 4.4: Results of the analyses performed on plant 2

Sample Type	Number of Positive samples	Total Samples Collected	Percentage of Positive samples out of total number of sample type	Total Percentage of positive samples out of total samples collected
Trunk	0	0	0%	0%
Cane	3	6	50%	11%
Petiole	0	6	0%	0%
Leaf	1	8	13%	4%
Root	0	7	0%	0%
Total	4	27	15%	

Table 4.5: Percentage of positive samples for each plant and final total per sample type

	Trunk	Cane	Leaf	Petiole	Root
Plant 7	22%	33%	20%	13%	0%
Plant 4	43%	43%	15%	0%	17%
Plant 2	-	15%	13%	0%	0%
Total	31%	40%	17%	5%	6%

Phloem scrapings from the cane samples yielded more positive results in comparison to the other sample types. Root and petiole samples yielded the lowest. Phloem scrapings from the trunk samples yielded the second highest percentage of positive results.

The distribution within individual plants presented no discernable pattern and appears to be erratic. Figure 4.7 shows a drawing of plant 4. The red sections show where Aster Yellows phytoplasma was detected.

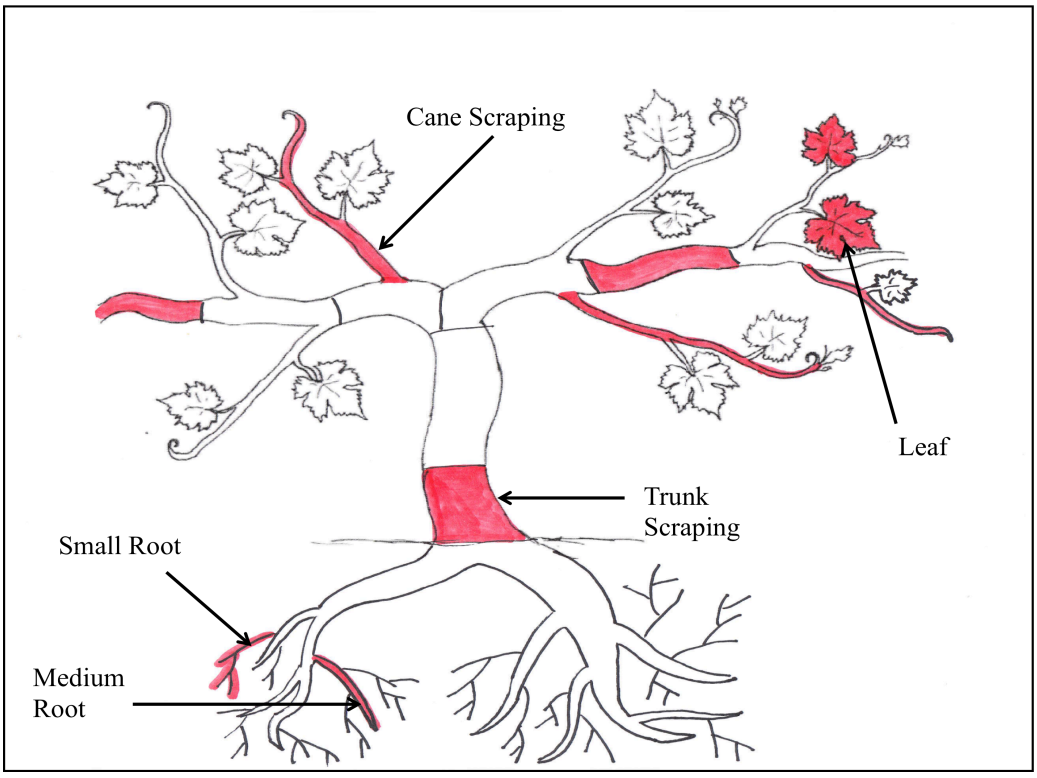

Figure 4.7: A drawing depicting the distribution of Aster Yellows phytoplasma in the individual plant (plant 4). Red areas are where the pathogen was detected by nested PCR.

4.3.4 Sequence Validation

Table 4.6 shows the first match obtained through a nucleotide BLAST of the sequences.

Table 4.6: Results of a nucleotide BLAST analysis performed on sequences validating the amplicons obtained for the spatial distribution represent Aster Yellows phytoplasma gene sequences

Description	Max Score	Total Score	Query cover	E Value	Identity	Accession
Aster yellows phytoplasma strain RzW14 16S ribosomal RNA gene, partial sequence; 16S-23S ribosomal RNA intergenic spacer and tRNA-Ile gene, complete sequence	1807	1807	100%	0.0	98%	HM561990.1

4.4 Discussion and Conclusion

The uneven distribution of phytoplasmas within the host plant has been widely suggested, yet little research is available, particularly in grapevines. South Africa is one of the leading producers of grape related products and as the recently identified Aster Yellows phytoplasma threatens vineyards in the country, accurate diagnostic protocols are paramount. This could ultimately lead to control of the disease.

The aim of this research chapter was to determine where in the grapevine host, phytoplasma is most abundant, thereby contributing to research into accurate diagnosis. Three whole-plants were removed from a vineyard in Vredendal, South Africa. Using nested PCR, different parts of the plant were tested for Aster Yellows phytoplasma. Real-Time PCR assay was not used for diagnosis as the titers were too low and negative results for several samples were observed (figure 4.5). These same samples were used in a nested PCR, of which 5 samples yielded positive results. Three of these amplicons were sequenced using Sanger Sequencing and once analysed through nucleotide BLAST, were confirmed to be Aster Yellows phytoplasma 16S ribosomal RNA (table 4.6).

Following verification , the rest of the samples were analyzed using nested PCR. The results of plant 7 are in table 4.2. Only 18% of the samples obtained from this grapevine plant yielded positive results. The sample type that yielded the most positive results was the cane samples with 33% of the total phloem scrapings from the cane being positive for phytoplasma infection. The phloem scrapings obtained from the trunk samples showed the second highest number of positive samples. Plant 4 showed equal percentage of positive results from the phloem scraped off both the trunk and cane samples. The cane samples obtained from plant two showed 50% positive results. Overall, (table 4.6) cane samples presented the optimal sample to collect for accurate phytoplasma infection, keeping in mind that phytoplasma was detected in all of the sample types collected, strengthening the theory that the pathogen can be found throughout the grapevine plant. These results do not correspond with those obtained by Christensen *et al* (2004) and Terlizzi and Credi (2007), whose research concluded that the optimal samples to collect were petioles and leaves, respectively. However, these studies did not involve Aster Yellows phytoplasma specifically within a grapevine plant.

The number of positive samples obtained from all three plants was lower than expected, despite the fact that all three plants showed strong symptoms in the field. The low titers of

phytoplasma infection can be further validated as detection was only possible after a third round of amplification during the nested PCR and that the Real-Time PCR was unable to detect any infection. Thus the low number of positive results could be attributed to such low titers that PCR was unable to sufficiently amplify the target sequence. Collection date may also have contributed to the low titers. October is very early in the growing season, so shoots and leaves were still relatively young. Nevertheless, Aster Yellows phytoplasma is known to have very low infection titers in woody plants, especially grapevines, making it difficult to detect.

Aster Yellows phytoplasma is also notorious for erratic distribution. Figure 4.7 is a sketch of plant 7 and shows where in the plant the phytoplasma was detected using nested PCR. The infection is inconsistent and no discernable pattern can be seen. Leaf samples yielded positive results, but their corresponding petioles and canes were negative. This may also be due to the very low titer, and that samples that appeared to be negative may not have been truly negative.

Figure 4.7 also illustrates the fact that phytoplasmas are found throughout the plant, including the root samples. The insect vector, namely the leafhopper, is a phloem feeding insect and feeds on the leaves of grapevine plants (Weintraub and Beanland, 2006). Therefore, the phytoplasma is able to move within the plant. Wei *et al* (2004) performed a study on the movement of phytoplasmas within *Glebionis coronaria* (garland chrysanthemum) and found that when a leafhopper inoculates phytoplasma in a leaf, the pathogen is able to migrate throughout the plant and even into the roots in just 48 hours. The mechanism behind the movement is unknown; however the movement does occur in the direction of the phloem stream, specifically from source tissues to sink tissues (Constable *et al*, 2003; Schaper and Seemüller, 1984). Source tissues are the source of the nutrients whereas sink tissues are where the nutrients are absorbed. Phytoplasmas move slower than the solutes and are occasionally undetectable in the sink tissues as observed by Christensen *et al* (2004). There is no research to date on the movement of Aster Yellows phytoplasma in a grapevine. However it can be seen that movement is unarguable.

When referring back to diagnostics, it can be deduced that detecting Aster Yellows phytoplasma in a grapevine plant using one type of tissue may not yield the most accurate results. It is therefore suggested to sample canes with their leaves and corresponding petioles. Phloem scrapings from the trunk are not optimal due to the difficulty of the sampling process. This study concludes that phloem scrapings from the canes yield the most positive results in

comparison to other sample types obtained from an infected plant, however even with these canes, negative diagnoses are possible. Cane samples are easily transported, and in experience diagnosis is reliable and reproducible.

4.5 References

Carstens R (2014) The incidence and distribution of grapevine yellows disease in South African vineyards. MSc Thesis. Stellenbosch University

Christensen NM, Nicolaisen M, Hansen M, Schulz A (2004) Distribution of Phytoplasmas in Infected Plants as Revealed by Real-Time PCR and Bioimaging. Molecular Plant Microbe Interactions 17 (11): 1175-1184

Constable FE, Gibb KS, Symons RH (2003) Seasonal distribution of phytoplasmas in Australian grapevines. Plant pathology 52: 267-276

Del Serrone P, Barba M (1996) Importance of the vegetative stage for phytoplasma detection in yellow-diseased grapevines. Vitis 35:101-102

Gibb KS, Constable FE, Moran JR, Padovan AC (1999) Phytoplasmas in Australian grapevines – detection, differentiation and associated diseases. Vitis 38 (3): 107-114

Osler R, Loi N, Refatti E (1995) Present knowledge on phytoplasma disease of fruit trees and grapevine. 2nd Slovenian Conference on Plant Protection in Radenci: 27-46

Schaper U, and Seemüller E (1984) Recolonization of the stem of apple proliferation and pear decline-diseased trees by the causal organisms in spring. Z. Pflanzenkrankh. Pflanzenschutz 91:608-613

Spinas N. (2012) The efficacy of the antimicrobial peptides D4E1, VvAMP-1 and Snakin1 against the grapevine pathogen aster yellows phytoplasma. MSc Thesis. Stellenbosch University

Terlizzi F, Credi R (2007) Uneven distribution of stolbur phytoplasma in Italian grapevines as revealed by nested-PCR. Bulletin of Insectology 60 (2): 365-366

Wei W, Kakizawa S, Suzuki S, Jung H-Y, Nishigawa H, *et al* (2004) In planta dynamic analysis of onion yellows phytoplasma using localized inoculation by insect transmission. Phytopathology 94:244–50

Weintraub PG, Beanland L (2006) Insect vectors of phytoplasma. Annual Review of Entomology. 51: 91-111

Chapter 5
Temporal Distribution and the occurrence of recovery of Aster Yellows phytoplasma in grapevine

5.1. Introduction

Phytoplasmas are notorious for erratic infection characteristics, with titers changing over time making it exceptionally difficult for accurate diagnosis and research. There are several theories as to why this happens; the possible seasonal/temporal distribution as well as the occurrence of recovery. In order to fully understand these patterns, scientists have delved into the research of distribution in order to determine the best time of year during which to detect phytoplasma infection accurately in crops all around the world.

Terlizzi and Credi (2007) proved that certain phytoplasma diseases such as Bois Noir was present in grapevine more often in the Italian summer seasons. It has been proposed that optimal detection of phytoplasmas in the summer months suggests seasonal titer fluctuations (Constable *et al,* 2003). For accurate diagnosis of Australian Grapevine Yellows phytoplasma, sampling should occur during January or February, when temperatures are at their highest and when symptom expression is greatest. From March onwards, the reliability of diagnosis decreases (Constable *et al*, 2003). In 1999, Gibb *et al* performed a temporal analysis using nested PCR on Australian grapevines in order to determine when the optimal time of year to detect phytoplasmas was. Their results are summarized in table 5.1. Grapevines sampled in the beginning and end of the season were shown to be negative in this study, whereas mid-season sampling exhibited positive results. The authors concluded that the months of greatest phytoplasma infection coincided with the warmest temperatures of the year (Gibb *et al*, 1999). It was also found that several grapevines diagnosed as positive for infection in one month, appeared to be negative in the following month. It was suggested that this was due to the uneven distribution of the pathogen throughout the grapevine plant (Gibb *et al*, 1999). When Grapevine Yellows disease was first detected in Australia, it was shown that Australian Grapevine Yellows disease was primarily found in the inland districts of New South Wales where the climate was noticeably warmer in comparison to other viticultural regions in the country (Constable *et al*, 2004).

Table 5.1: Results of a temporal distribution of phytoplasma infection in Australian grapevines (Gibb *et al,* 1999)

Month sampled	Number of Positives in 1995/96 (Total=20)	Number of Positives in 1996/97 (Total=20)
October	Not tested	1
November	Not tested	9
December	0	9
January	10	15
February	14	7
March	6	0
April	0	0
May	Not tested	0

Not only are there hypotheses of varying infection titer over time periods, there have also been observations where infections in vineyards have cumulatively increased over seasons (Batlle *et al*, 2000). Using nested PCR to detect Bois Noir in Spanish vineyards, Batlle *et al* (2000) observed an increase in incidence from 3.4% in 1994 to 18.4% in 1997. These results suggest that the titer of phytoplasma infection increases over time. A survey was performed over a period of four years where the yearly incidence of Aster Yellows phytoplasma was tested in Chardonnay grapevines. It was found that the yearly cumulative incidence was 37% and it was suggested that if no control was established, 100% of the vines would be diseased in ten years time (Carstens, 2014). This yearly increase is not perpetual, as there have been reports where phytoplasma infected plants, including grapevines, have shown unforced remission of symptoms and appear to be healthy again (Caudwell, 1961; Osler *et al*, 1999; Musetti *et al,* 2004, 2005).

This spontaneous remission of phytoplasma symptoms is described as the recovery phenotype phenomenon (Caudwell, 1961). The previously infected plant presents with no symptoms linked with phytoplasma infection. This was first observed in France and Italy in grapevines that were infected with Flavescence dorée (grapevine yellows disease) (Caudwell, 1961). There have been a number of hypotheses regarding how recovery occurs, one of which proposes the increase of hydrogen peroxide in the plants. Further research showed abundance of hydrogen peroxide in the phloem of recovered grapevine plants, but not in that of the

healthy nor diseased plants (Musetti *et al*, 2004). Several other stresses such as grafting, cutting back and replanting have also shown to induce recovery (Osler *et al*, 1993). This revival of infected plants can be permanent or temporary, and is considered to be in permanent recovery when Aster Yellows phytoplasma symptoms have not been displayed for three consecutive years (Maixner, 2006). By inducing recovery phenotype by means of pruning, a technique already in practice in South Africa, it may be possible to control the titer of Aster Yellows phytoplasma in grapevines, however this theory has not been scientifically proven and no data supporting the practice has been published to date.

Due to the pathogen's titer changing over time, precise diagnosis requires research into the temporal distribution of the pathogen. Further research is required to accurately determine the optimal time of year to study and diagnose the occurrence of Aster Yellows phytoplasma in grapevines. Research into methods of control can be equally as vital, which is why the hypothesis of inducing recovery through pruning practices is further studied.

5.2. Materials and Methods

5.2.1 Sample Collection

Samples were collected from Vredendal, South Africa. In January 2013, leaf and its corresponding petiole samples were taken from plants (Chardonnay cultivar) that displayed symptoms typical of Aster Yellows phytoplasma, namely the yellowing of leaves, aborted bunches, growth of axillary shoots etc. The symptomatic leaf and petioles were randomly obtained off the plant, purely dependent on where the symptom expression was highest. The samples were flash frozen in the field using liquid nitrogen and transported back to the laboratory on dry ice.

To determine temporal distribution, samples were collected at different time points during the growing season, specifically once a month from January to March 2013 and again in November 2013 to March 2014. During the first collection (January 2013), chosen vines were labelled and location was noted in order to refer back to the same plants for each collection. Symptoms expressed by the plants at each sampling date were recorded. Samples were stored at -80 ^{o}C.

Samples were also collected from grapevine plants cv Chenin blanc that were pruned back 2 years prior to the first collection date. These plants had ceased showing symptoms and were

classified as being in recovery. A total of 50 samples were collected from separate plants in the same vineyard and were collected in February 2013 and February 2014. In January 2013, 20 young grapevine plants (cv Chenin blanc) were placed among the 50 plants that were in recovery. These 20 plants were confirmed not to be infected with Aster Yellows phytoplasma and were placed in the vineyard in order to determine a re-infection rate. All collected plant samples were stored at -80 ºC until tested.

5.2.2. Sample Preparation and DNA Extraction

Leaf samples were macerated into a fine powder using liquid nitrogen in a mortar and pestle. The Nucleospin Plant II DNA Extraction kit was used with 0.1g of ground material. Quality of the DNA was determined by gel electrophoresis and Nanodrop.

5.2.3. Diagnostics

Both nested PCR and the Real-Time PCR assays were used to screen the samples for Aster Yellows phytoplasma infection. See protocols in sections 3.2.1 and 3.2.2.2, respectively.

A positive control previously diagnosed with Aster Yellows phytoplasma was used with a plant negative and a no template control to ensure no contamination.

Final products of the nested PCR were analyzed by electrophoresis through a 1% agarose gel with ethidium bromide and visualized using a UV transilluminator.

5.2.4. Sequence Validation

Several positive amplicons were excised from gels, purified using Zymoclean™ Gel DNA Recovery Kit and sequenced using Sanger Sequencing. Sequences were analyzed using BLAST to confirm the identity of Aster Yellows phytoplasma.

5.3. Results

5.3.1 DNA Extraction

DNA extractions yielded concentrations ranging from 20 ng/µL to 60 ng/µL. The required concentration for nested PCR falls between this range, however, for consistency samples were diluted with MilliQ water to 20 ng/µL.

3.3.2 Temporal Distribution

After testing samples with Real-Time PCR it was determined that the infection titer of Aster Yellows phytoplasma was too low to be detected with this assay (Figure 5.1). The standard sample amplified but the unknowns remained negative. This could be due to the presence of PCR inhibitors or the lower sensitivity of this assay as determined in chapter 3.

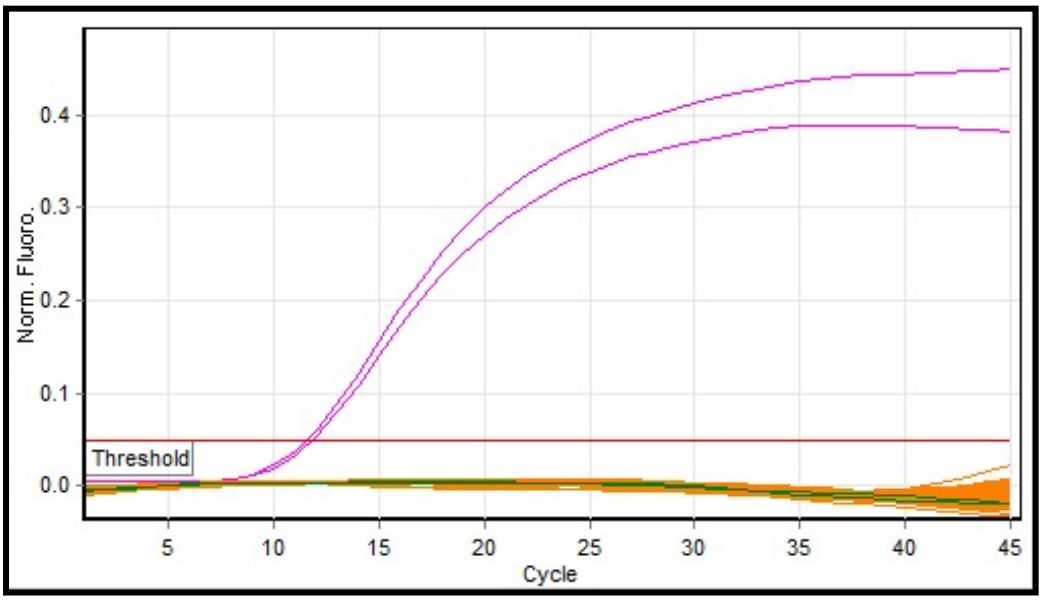

Figure 5.1: Amplification profile of the samples collected in February 2014. Pink represents the plasmid control, orange represents all of the unknown samples and green represents the no template control.

The nested PCR assay was subsequently used and yielded significantly more positives (Figure 5.2).

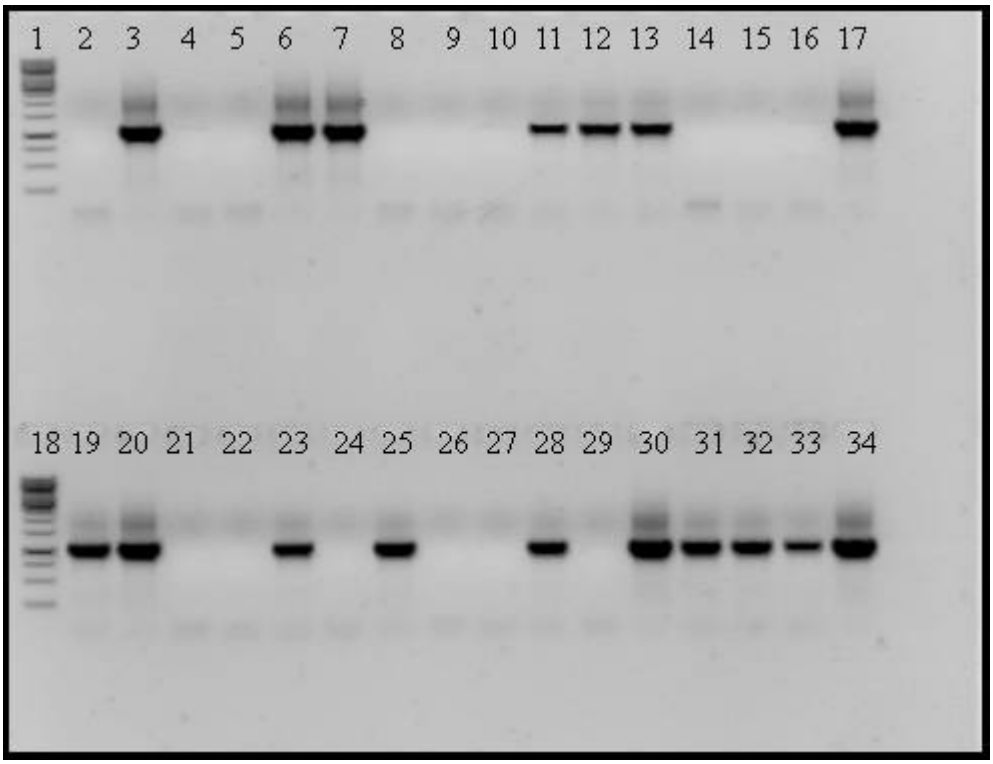

Figure 5.2: Agarose gel of nested PCR products from February 2014. Lane 1&18, 1 kb marker. Lane 2, No template control. Lane 3, Positive control. Lanes 4-17 & 19-34, unknown samples.

The final results are shown in table 5.2. The number of plants displaying positive results is shown. The percentage of positive plants is also shown, and is depicted in the graph in figure 5.3.

Table 5.2: Results of the temporal distribution of Aster Yellows phytoplasma in grapevines.

Month	Number of positive plants out of 30 selected	Percentage of positive plants (%)
January 2013	5	16.7
February 2013	8	26.7
March 2013	5	16.7
November 2013	5	16.7
December 2013	7	23.3
January 2014	6	20.0
February 2014	16	53.3
March 2014	7	23.3

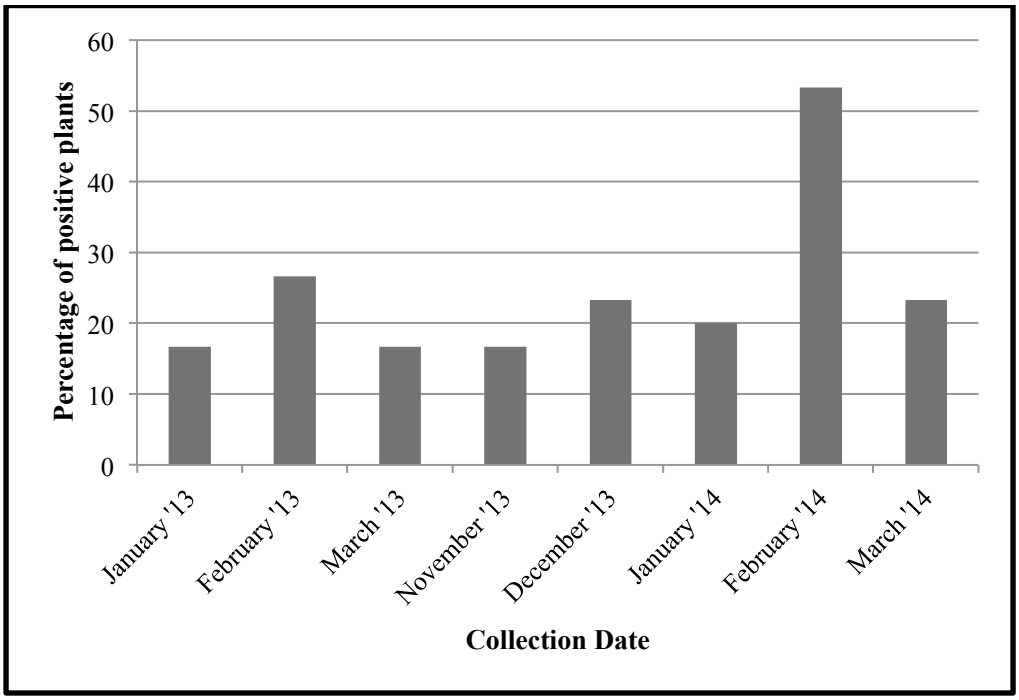

Figure 5.3: A Bar graph depicting the percentage of positive plants collected at the specific time points showing the temporal distribution of Aster Yellows phytoplasma.

After screening the 30 plants collected at 8 different time points, it was noted that plants diagnosed with Aster Yellows phytoplasma were not consistent throughout the season. Table 5.3 shows the plants that were identified as positive for the pathogen at least once and how they may not necessarily be positive in the subsequent months.

Table 5.3: Individual results of each plant in which Aster Yellows phytoplasma was identified and when the pathogen was detected. The shaded blocks represent a positive diagnosis. (Note: Four samples collected were negative for infection at every time point and are not shown in the table)

Plant Name	2013					2014		
N6	Jan	Feb	March	Nov	Dec	Jan	Feb	March
N7	Jan	Feb	March	Nov	Dec	Jan	Feb	March
P74	Jan	Feb	March	Nov	Dec	Jan	Feb	March
N8	Jan	Feb	March	Nov	Dec	Jan	Feb	March
P84	Jan	Feb	March	Nov	Dec	Jan	Feb	March
P102	Jan	Feb	March	Nov	Dec	Jan	Feb	March

Plant Name	2013					2014		
N6	Jan	Feb	March	Nov	Dec	Jan	Feb	March
N7	Jan	Feb	March	Nov	Dec	Jan	Feb	March
P74	Jan	Feb	March	Nov	Dec	Jan	Feb	March
N8	Jan	Feb	March	Nov	Dec	Jan	Feb	March
P84	Jan	Feb	March	Nov	Dec	Jan	Feb	March
P102	Jan	Feb	March	Nov	Dec	Jan	Feb	March
P104	Jan	Feb	March	Nov	Dec	Jan	Feb	March
P105	Jan	Feb	March	Nov	Dec	Jan	Feb	March
P112	Jan	Feb	March	Nov	Dec	Jan	Feb	March
P114	Jan	Feb	March	Nov	Dec	Jan	Feb	March
P87	Jan	Feb	March	Nov	Dec	Jan	Feb	March
N3	Jan	Feb	March	Nov	Dec	Jan	Feb	March
P117	Jan	Feb	March	Nov	Dec	Jan	Feb	March
P89	Jan	Feb	March	Nov	Dec	Jan	Feb	March
P129	Jan	Feb	March	Nov	Dec	Jan	Feb	March
P130	Jan	Feb	March	Nov	Dec	Jan	Feb	March
N1	Jan	Feb	March	Nov	Dec	Jan	Feb	March
N2	Jan	Feb	March	Nov	Dec	Jan	Feb	March
N9	Jan	Feb	March	Nov	Dec	Jan	Feb	March
N12	Jan	Feb	March	Nov	Dec	Jan	Feb	March
P94	Jan	Feb	March	Nov	Dec	Jan	Feb	March
N10	Jan	Feb	March	Nov	Dec	Jan	Feb	March
N11	Jan	Feb	March	Nov	Dec	Jan	Feb	March
N13	Jan	Feb	March	Nov	Dec	Jan	Feb	March
N15	Jan	Feb	March	Nov	Dec	Jan	Feb	March
N16	Jan	Feb	March	Nov	Dec	Jan	Feb	March

For both years, February had the most positive samples out of the 30 collected each month. It is important to note that symptoms were observed throughout collection times, however more noticeably in December 2013. Figure 5.4 shows leaves from a vine previously detected as infected (A) compared to a leaf collected from a vine used as a negative control (B). The progression of the yellowing of the leaves in the infected plant is evident. The leaves (A) were also very brittle and were starting to roll downward. These symptoms are strong identifiers for Grapevine Yellows disease. In January of 2013 and February of 2014, symptoms were present, yet distinguishing symptomatic leaves from leaves that were perishing from old age proved difficult. The environmental conditions such as high temperatures and a dry climate could contribute to deterioration of the leaves.

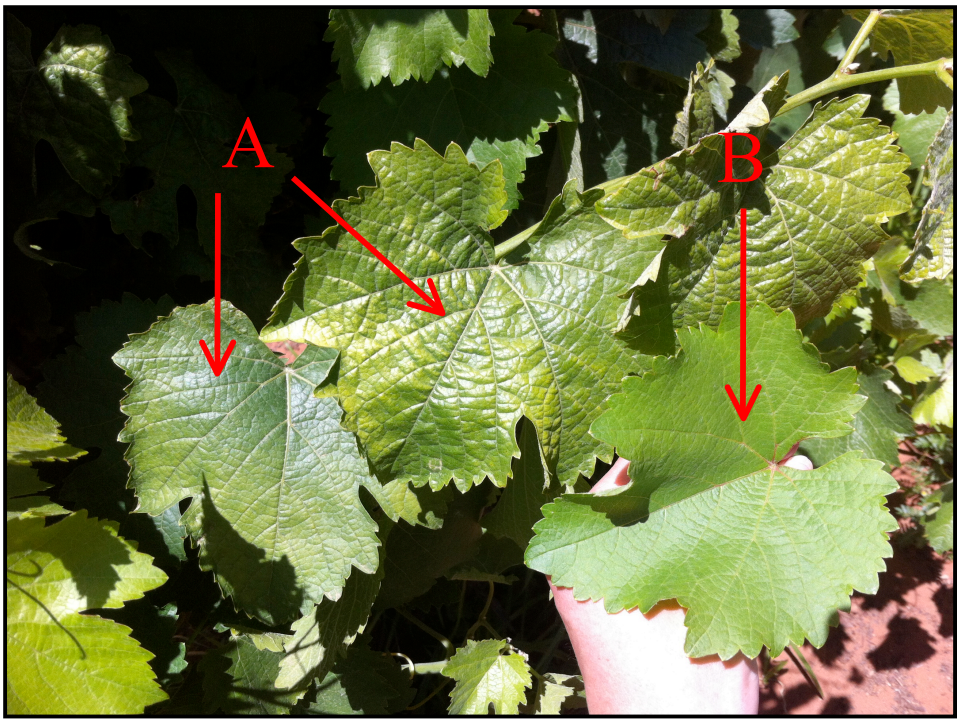

Figure 5.4: Photograph comparing the Aster Yellows phytoplasma symptom expression in a leaf of one of the plants sampled to a healthy leaf. (A) Shows a plant previously diagnosed and infected whereas (B) shows a leaf from a plant used as a negative control.

Samples that yielded positive results were tested again to rule out contamination, and sequenced in order to validate the amplicons were in fact Aster Yellows phytoplasma. The first three sequence matches that resulted from the nucleotide BLAST are shown in the table 5.4.

Table 5.4: The first three matches resulting of a nucleotide BLAST analysis performed on sequences validating amplicons represent Aster Yellows phytoplasma gene sequences.

Description	Max Score	Total Score	Query cover	E Value	Identity	Accession
Aster yellows phytoplasma strain RzW14 16S ribosomal RNA gene, partial sequence; 16S-23S ribosomal RNA intergenic spacer and tRNA-Ile gene, complete sequence	1807	1807	100%	0.0	98%	HM561990.1
Aster yellows phytoplasma strain AY-J 16S ribosomal RNA gene, partial sequence; and tRNA-Ile gene, complete sequence	1807	1807	100%	0.0	98%	HM590616.1
Aster yellows phytoplasma strain AY-27 16S ribosomal RNA gene, partial sequence; tRNA-Ile gene, complete sequence; and 23S ribosomal RNA gene, partial sequence	1807	1807	100%	0.0	98%	HM467127.1

3.3.2 Recovery Phenotype

All samples collected and tested using the nested PCR procedure yielded negative results (not shown) for both time points (February 2013/14). Positive and negative controls produced expected results, thus negative results cannot be attributed to failed PCR reactions.

3.4. Discussion and Conclusion

Accurate diagnosis of Aster Yellows phytoplasma can be difficult due to the change of infection titer over seasons. In order to fully understand the pathogen, it was necessary to determine the time of year for most accurate diagnosis of this phytoplasma.

After testing 30 plants using nested PCR over one and a half growing seasons, it was determined that more plants showed positive diagnoses in February than in any other month (Table 5.2 and Figure 5.2). In 2013, 27% of plants were positive for Aster Yellows phytoplasma in February. In January, March and November, 17% of the 30 plants collected were positive, with an increase to 23% observed in December. In 2014, February again presented the most positive plants, with 53% of the plants being positive for infection. There are many factors that may affect the distribution of phytoplasma infection over time. These factors may include the change of climate over the season, vector behaviour and possible infection of other plant diseases. In the Western Cape province of South Africa, January and February are the hottest months of the year. The results of this study then correspond to those published by Gibb *et al* in 1999 where phytoplasma infection was the highest during the hottest times of the year. There are many possible reasons as why there is an erratic temporal distribution of phytoplasmas in their host plants. Gibb *et al* (1999) proposed variation of phytoplasma infection in grapevines may be affected by recent inoculation events. The change in environment due to climate and temperature could influence the rate of circulation of nutrients and thus possibly phytoplasma within the plant. Alternatively, phytoplasma infection may not change over one season, but chemicals that could affect and inhibit PCR reactions may vary over time, but this is improbable as these chemicals were most likely eliminated by dilutions.

The increase in percentage of infection in 2014 was noticeable. January, February and March showed more positive plants than in 2013, suggesting that the infection increased over time, similar to what was reported for Bois Noir by Batlle *et al* in 2000. This may be due to further inoculation events adding to the multiplication of the pathogens within the plant.

Even though symptoms are present and change from month to month, they may not be an indication of pathogen titer. Symptoms in the vineyard, where the 30 plants were sampled, showed more noticeable symptoms in December compared to the other collection time points. Several plants exhibiting symptoms yielded negative results. Table 5.2 illustrates the erratic changes in infection each plant displayed. A particular plant may show a positive diagnosis at one time point, however a negative result at the following time point. This reflects the uneven and erratic distribution of phytoplasma infection within the plant. It is important to note that phytoplasma titers in grapevines are notoriously low thus negative results may be due to such low titers that diagnostic procedures are unable to detect the pathogen.

In 2011, 50 grapevine plants displaying symptoms for Aster yellows phytoplasma infection were pruned back. These plants were classified as in recovery as symptom expression ceased. These plants were sampled in February of 2013 and 2014, and after analysis by nested PCR, all plants were diagnosed as negative for Aster Yellows phytoplasma infection. There was no symptom expression at collection time points. This again may be attributed to phytoplasma titers being too low to detect. It may be necessary to continue analysis for a further season to validate negative results.

Due to the difficulty of detecting phytoplasma, it is vital to determine the time of year in which it is optimal to diagnose infection. This study has determined that accurate diagnosis is possible in February, or in the middle of the growing season. Not only will this research benefit farmers, it will give insight for further studies involving reliable diagnosis and prevention and control of Aster Yellows phytoplasma.

3.5. References

Batlle A, Martinez MA, Lavina A (2000) Occurrence, distribution and epidemiology of Grapevine Yellows in Spain. European Journal of Plant Pathology 106: 811–816

Caudwell, A (1961) Les phénomènes de rétablissement chez la flavescence dorée de la vigne. Annales des Epiphyties 12: 347-354

Constable FE, Jones J, Gibb KS, Chalmers YM, Symons RH (2004) The incidence, distribution and expression of later season leaf curl diseases in selected Australian vineyards. Annual applied Biology 144: 205-218

Constable FE, Gibb KS, Symons RH (2003) Seasonal distribution of phytoplasmas in Australian grapevines. Plant pathology 52: 267-276

Deng S, Hiruki C (1991) Amplification of 16S rRNA genes from culturable and nonculturable mollicutes. Journal of Microbiological Methods 14:53-61

Gibb KS, Constable FE, Moran JR, Padovan AC (1999) Phytoplasmas in Australian grapevines – detection, differentiation and associated diseases. Vitis 38 (3): 107-114

Gundersen DE, Lee I-M (1996) Ultrasensitive detection of phytoplasmas by nested-PCR assays using two universal primer pairs. Phytopathologia Mediterranea 35:144-151

Lee I-M, Gundersen DE, Hammond RW, Davis RE (1994) Use of mycoplasmalike organism (MLO) group-specific oligonucleotide primers for nested-PCR assays to detect mixed-MLO infections in a single host plant. Phytopathology 84:559-566

Lee I-M, Hammond RW, Davis RE, Gundersen DE (1993) Universal amplification and analysis of pathogen 16S rDNA for classification and identification of mycoplasmalike organisms. Phytopathology 83:834-842

Musetti R, Marabottini R, Badiani M, Martini M, Sanitá di Toppi L, Borselli S, Borgo M, Osler R (2007) On the role of H2O2 in the recovery of grapevine (*Vitis vinifera* cv. Prosecco) from Flavescence dorée disease. Functional Plant Biology 34: 750-758

Musetti R, Sanita di Toppi L, Ermacora P, Favali MA (2004) Recovery in apple trees infected with the apple proliferation phytoplasma: an ultrastructural and biochemical study. Phytopathology 94, 203–208

Musetti R, Sanita di Toppi L, Martini M, Ferrini F, Loschi A, Favali MA, Osler R (2005) Hydrogen peroxide localisation and antioxidant status in the recovery of apricot plants from European stone fruit yellows. European Journal of Plant Pathology 112, 53–61

Maixner M (2006) Temporal behaviour of grapevines infected by type II of Vergilbungskrankheit (Bois noir). Extended Abstracts 15th Meeting of ICVG Stellenbosch 2006: 223-224

Osler R, Carraro L, Loi N, Refatti E (1993) Symptom expression and disease occurrence of a yellows disease of grapevine in northeastern Italy. Plant Disease 77: 496-498

Osler R, Loi N, Carraro L, Ermacora P, Refatti E (1999) Recovery in plants affected by phytoplasmas. In 'Proceedings of the 5th Congress of European Foundation for Plant Pathology'. (Ed. Societa Italiana di ` Patologia Vegetale) 589–592 (Taormina, Italy)

Schneider B, Seemuller E, Smart CD, and Kirkpatrick BC (1995) Phylogenetic classification of plant pathogenic mycoplasma-like organisms or phytoplasmas. Pages 369-380 in: Molecular and Diagnostic Procedures in Mycoplasmology, vol. I. S. Razin and J. G. Tully, eds. Academic Press, New York, USA

Terlizzi F, Credi R (2007) Uneven distribution of stolbur phytoplasma in Italian grapevines as revealed by nested-PCR. Bulletin of Insectology 60 (2): 365-366

Chapter 6
General Conclusion

The aim of this study was to determine the spatial and temporal distribution of Aster Yellows phytoplasma in grapevines in South Africa. The recovery phenotype phenomenon was also investigated to observe whether pruning practises are able to induce recovery and if this recovery is permanent. To perform this research, a reliable assay was required.

Three different PCR assays were compared using the same dilution series. Two of these were Real-Time PCRs with absolute quantification. The first assay used Syto9 as a double stranded DNA specific dye in combination with previously designed primers (Visser, 2011). The second assay utilized a TaqMan® Probe and primers designed by Hodgetts *et al* (2009). This assay was also a multiplex PCR with an endogenous control to ensure efficient PCR amplification. This assay proved to be more sensitive when detecting low titers of Aster Yellows phytoplasma in grapevines. Nevertheless, it was still not sensitive enough, as samples collected for both the spatial and temporal distribution experiments tended to show very low pathogen titers. The third assay used in the comparison was a nested PCR with 3 amplification steps using universal primers. This assay was able to detect the lowest titers in comparison to the Real-Time PCRs and was used for sample analyses. Unfortunately, one is unable to quantify pathogen titers with nested PCR, thus future prospects should include development of a new Real-Time PCR assay, optimized specifically for Aster Yellows phytoplasma in grapevines. Quantification is a vital element that contributes to accurate diagnosis and further understanding of many plant pathogens, including the phytoplasmas.

One of the many obstacles to overcome with phytoplasma diagnostics is the varying pathogen titers in different sections of the plant. Different samples (leaf, petiole, trunk, cane and roots) were analysed from whole grapevines known to be infected with Aster Yellows phytoplasma. Phloem scrapings obtained from the cane samples yielded the most positive results in comparison to the other sample types collected. Therefore, it can be suggested that for accurate diagnosis, sampling the canes of symptomatic grapevines would be reliable. It is important to note, however, that the sampling of these whole plants took place in October, the beginning of the growing season. In order to fully understand the spatial distribution of Aster Yellows phytoplasma in grapevines, one should sample whole plants throughout the growing season and determine whether the patterns change over time.

The temporal distribution of Aster Yellows phytoplasma in grapevine was investigated over two growing seasons. Leaf and petiole samples were collected from 30 grapevines at specific time points, and it was determined that February, for both seasons, yielded the most positive results. It was hypothesized that climate has an effect on infection titer as February showed the highest temperatures in the regions from which samples were obtained. Results did not correlate with symptom expression, as plants exhibited strong symptoms during the December 2013 collection. Results also suggested an increase of infection over seasons. It is, however, necessary to continue this study for several seasons in order to validate findings and perhaps determine a rate at which infection increases. This may yield greater insight into how the pathogen spreads and thus preventing the dispersion.

Pruning practices in South Africa is commonly used to prevent the spread of Aster Yellows phytoplasma as it can induce a recovery phenotype. The final aim of this study was to determine if the recovery is temporary or permanent. The samples collected in both seasons from plants previously pruned back yielded negative results for infection, adding to the weight of the argument of pruning. The definite shortcoming of this study was the low pathogen titers experienced in samples collected. These low titers together with the theory that infection increases over time, supports the continuation of testing the pruned plants, as Aster Yellows phytoplasma may still be present in the grapevines.

This research contributed to our understanding of diagnosis of Aster Yellows phytoplasma in grapevine. It can be deduced that for accurate detection, cane samples should be collected. Should leaf and petioles be sampled, February or during the warmest climates of the season would be the best time. Perfecting the diagnosis of Aster Yellows phytoplasma in grapevines can lead to advancements in prevention and control of this devastating pathogen.

References

Hodgetts J, Boonham N, Mumford R, Dickinson M (2009) Panel of 23S rRNA gene-based Real-Time PCR assays for improved universal ad group-specific detection of phytoplasmas. Applied and Environmental Microbiology 75 (9): 2945-2950

Visser M (2011) An evaluation of the efficacy of antimicrobial peptides against grapevine pathogens. MSc thesis. Department of Genetics, Stellenbosch University